

## CRITICAL REVIEW

View Article Online  
View Journal | View Issue



Cite this: *Environ. Sci.: Atmos.*, 2026, 6, 754

## The global atmospheric cycle of forever chemicals: a review of PFAS distribution, wet deposition, and atmospheric fate

Youssef Harb, <sup>†‡</sup><sup>a</sup> Charbel Anthony El Hachem,<sup>‡</sup><sup>b</sup> Amale Mcheik,<sup>a</sup> Ghada El Zakhem Naous <sup>a</sup> and Nathalie Hayeck <sup>\*a</sup>

Per- and polyfluoroalkyl substances (PFAS) are persistent, emerging environmental contaminants with diverse chemical properties and widespread industrial and consumer uses. They are used as key components in products like surfactants, lubricants, fire-fighting foams, non-stick cookware, and water-repellent coatings. Additionally, their volatility and stability enable global transport, often reaching pristine environments across various regions. This review thoroughly examines the global literature on atmospheric PFAS, focusing on their distribution in polar, midlatitude, and tropical areas, the role and mechanisms of wet deposition in their atmospheric behavior, and their chemical transformation and phase partitioning in the atmosphere. While midlatitude industrial and consumer activities are primary sources, PFAS are transported globally. Moreover, wet deposition acts as a sink for atmospheric PFAS, with snow and sea spray especially effective at scavenging long-chain PFAS. Although secondary emissions through re-volatilization could occur, the main factors governing the fate of atmospheric PFAS are precursor transformations and phase partitioning. Volatile PFAS degrade in the atmosphere into more persistent and less volatile forms *via* oxidative and photochemical processes. The partitioning of PFAS between gas and particulate phases depends on functionalization and chain length, with some studies also emphasizing the role of meteorological conditions. Although this review covers a broad range of regions and environments, the existing literature remains limited, especially in areas such as the Antarctic Peninsula, the Middle East, Africa, and Latin America, where data gaps persist. Future research should focus on monitoring PFAS levels in these underrepresented regions and on enhancing the fundamental and mechanistic understanding of PFAS transformation pathways. Meanwhile, policymakers should prioritize implementing stricter emission controls, reforming regulations on legacy and precursor PFAS, and harmonizing PFAS regulations worldwide.

Received 7th October 2025  
Accepted 21st April 2026

DOI: 10.1039/d5ea00130g

rsc.li/esatmospheres

### Environmental significance

This review highlights the urgent need to address the widespread contamination of per- and polyfluoroalkyl substances (PFAS), commonly referred to as “forever chemicals”, which pose significant risks to ecosystems and human health due to their persistence and bioaccumulation. It highlights how industrial and consumer activities in midlatitude regions contribute substantially to PFAS emissions, which can reach remote areas, including pristine environments like the Arctic, through complex atmospheric processes and wet deposition. The findings underscore the need for stronger regulatory frameworks and enhanced monitoring, particularly in underrepresented regions, to better understand PFAS transport and mitigate their long-term effects. Addressing PFAS contamination is critical for safeguarding biodiversity, ecosystem integrity, and public health, necessitating urgent international collaboration.

## 1. Introduction

Per- and polyfluoroalkyl substances (PFAS) are a group of aliphatic molecules that are composed of hydrophobic carbon–fluorine backbone with a hydrophilic functionalized head.<sup>1</sup> The most popular definition of PFAS in the present literature was proposed by Buck *et al.*, in which PFAS are described as molecules with a backbone structure like that of an aliphatic hydrocarbon, but with hydrogen atoms replaced with fluorine atoms with the formula (C<sub>n</sub>F<sub>2n+1</sub>).<sup>2</sup> The general chemical

<sup>a</sup>Department of Physical Sciences, Lebanese American University, Chouran, Beirut 1102-2801, Lebanon. E-mail: Nathalie.hayeck@lau.edu.lb; Tel: +961 1 786456 Ext. 3412

<sup>b</sup>Department of Biological Sciences, Lebanese American University, Chouran, Beirut 1102-2801, Lebanon

<sup>†</sup> Now at Department of Chemistry, University of California, Irvine, California 92697, United States.

<sup>‡</sup> Both authors contributed equally to this review.



concept of “polyfluorination” includes compounds with several fluorine atoms that are either “scattered” or “grouped”.<sup>2</sup> However, not all polyfluorinated substances are considered PFAS as the presence of at least one perfluoroalkyl moiety is essential ( $C_nF_{2n+1}$ ).<sup>2</sup>

In 2018, the Organization for Economic Cooperation and Development (OECD) established a more precise and unified definition of PFAS in regulatory discussions.<sup>3</sup> The definition

involved considering a substance to be PFAS if it contains at least one of the following molecular structures:  $-C_nF_{2n}$  ( $n \geq 3$ ) or  $-C_nF_{2n}OC_mF_{2m}$  ( $n, m \geq 1$ ).<sup>3</sup> The former encompasses a fully fluorinated, known as polyfluorinated, carbon chain with at least three carbon atoms, and the latter involves a perfluorinated ether group with oxygen acting as a linker between the fluorinated carbon groups.<sup>3</sup> However, the OECD expanded this definition in 2021 by widening the scope of PFAS classification to include short-chain PFAS.<sup>4</sup> Moreover, in 2022, the United States Environmental Protection Agency (US EPA) modified a previously proposed definition that limited PFAS to compounds with at least two carbon atoms, one completely and another partially fluorinated.<sup>5</sup> This adjustment involved a broader definition that includes fluorocarbons with branched chains and fluoroethers.<sup>5</sup>

To facilitate discussion of atmospheric fate and transport, Table 1 lists representative PFAS compounds along with their nomenclature, CAS numbers, chain lengths, and classifications. PFAS could be categorized into two main categories: long-chain



Youssef Harb

*Youssef Harb is currently a PhD student at the University of California, Irvine, co-advised by Sergey Nizkorodov and Manabu Shiraiwa. He received his BS in Chemistry from the Lebanese American University, graduating as a valedictorian and receiving the Riyadh Nassar Leadership Award. His research focuses on atmospheric and environmental chemistry, aerosol processes, and the fate of emerging pollutants, with emphasis on their impact on human health.*



Charbel Anthony El Hachem

*Charbel Anthony El Hachem is currently a medical student at the University of Caen, Normandy. He completed two years of biology at the Lebanese American University, earning dean's distinction for 4 consecutive semesters. His research interest focuses on environmental health and toxicology, particularly the environmental deposition, bioaccumulation, and human health effects of per- and polyfluoroalkyl substances (PFAS).*



Amale Mcheik

*Dr Amale Mcheik is a post-doctoral researcher at the Lebanese American University. She received her PhD in Environmental Sciences from the University of Paris XII. Dr Mcheik's research focuses on the leaching of metals from soil into groundwater, soil and water pollution, and studies of many pharmaceutical plants.*



Ghada El Zakhem Naous

*Ghada El Zakhem Naous is a Senior Instructor of Chemistry in the Department of Physical Sciences at the Lebanese American University. She holds a BS and MS in Chemistry from the American University of Beirut. Her research focuses on food safety, toxicology, and environmental contaminants, particularly acrylamide and per- and polyfluoroalkyl substances (PFAS) in food, water, and atmospheric samples. She has published on dietary exposure risks from common Lebanese food products, with the aim of improving industrial processing and consumer health. Her work contributes to advancing public health and sustainability in the region.*



Nathalie Hayeck

*Dr Nathalie Hayeck is an assistant professor of chemistry in the Department of Physical Sciences at the Lebanese American University. She received her PhD in Environmental Chemistry from Aix-Marseille University in 2015. Dr Hayeck's expertise encompasses the study of volatile organic compounds (VOCs), the chemical aging of secondary organic aerosols (SOA), and the development of experimental setups to simulate atmospheric conditions. Her research aims to bridge the gap between molecular-level surface interactions and large-scale atmospheric observations. She has contributed significantly to the understanding of how light-induced reactions at the air–water interface influences the chemical composition of the troposphere.*



Table 1 Common names, IUPAC names, acronyms, CAS numbers, carbon chain lengths, and classifications of selected PFAS compounds<sup>a</sup>

Common name	IUPAC name	Acronym	CAS number	Carbon chain length	Classification
Trifluoroacetic acid	2,2,2-Trifluoroacetic acid	TFA	76-05-1	2	Ultrashort chain
Perfluoropropanoic acid	2,3,3-Tetrafluoropropanoic acid	PFPrA	359-49-9	3	Ultrashort chain
Perfluoropropanesulfonic acid	1,1,2,2,3,3,3-Heptafluoropropane-1-sulfonic acid	PFPrS	423-41-6	3	Ultrashort chain
Perfluorobutanoic acid	2,3,3,4,4-Hexafluorobutanoic acid	PFBA	62765-25-7	4	Short chain
Perfluorobutanesulfonic acid	1,1,2,2,3,3,4,4,4-Nonafluorobutane-1-sulfonic acid	PFBS	375-73-5	4	Short chain
Perfluoropentanoic acid	2,2,3,4,4,5,5,5-Octafluoro-3-(trifluoromethyl)pentanoic acid	PFPeA	64139-66-8	5	Short chain
Perfluoropentanesulfonic acid	1,1,2,2,3,3,4,4,5,5,5-Undecafluoropentane-1-sulfonic acid	PFPeS	2706-91-4	5	Short chain
Perfluorohexanoic acid	2,2,3,3,4,4,5,6,6-Decafluoro-5-(trifluoromethyl)hexanoic acid	PFHxA	15899-29-3	6	Short chain
Perfluorohexanesulfonic acid	1,1,2,2,3,3,4,4,5,5,6,6-Tridecafluorohexane-1-sulfonic acid	PFHxS	355-46-4	6	Short chain
2-(Perfluorobutyl)ethanol	3,3,4,4,5,5,6,6-Nonafluorohexan-1-ol	4 : 2 FTOH	2043-47-2	6	Short chain
Hexafluoropropylene oxide-dimer acid	2,3,3,3-Tetrafluoro-2-(1,1,2,2,3,3,3,3-heptafluoropropoxy)propanoate	HFPO-DA (GenX)	122499-17-6	6	Short chain
Perfluorooctanoic acid	2,2,3,3,4,4,5,5,6,6,7,7,8,8-Pentadecafluorooctanoic acid	PFOA	335-67-1	8	Long chain
Perfluorooctane sulfonate	1,1,2,2,3,3,4,4,5,5,6,6,7,7,8,8-Heptafluorooctane-1-sulfonate	PFOs	45298-90-6	8	Long chain
Perfluorooctanesulfonamide	1,1,2,2,3,3,4,4,5,5,6,6,7,7,8,8-Heptafluorooctane-1-sulfonamide	PFOSA	754-91-6	8	Long chain
N-Methylperfluorooctanesulfonamide	1,1,2,2,3,3,4,4,5,5,6,6,7,7,8,8-Heptafluoro-N-methyl-octanesulfonamide	MeFOsa	31506-32-8	8	Long chain
N-Ethylperfluorooctanesulfonamide	N-Ethyl-1,1,2,2,3,3,4,4,5,5,6,6,7,7,8,8-heptafluoro-1-octanesulfonamide	EtFOsa	4151-50-2	8	Long chain
N-Methylperfluorooctanesulfonamidoethanol	1,1,2,2,3,3,4,4,5,5,6,6,7,7,8,8-Heptafluoro-N-(2-hydroxyethyl)-N-methyl-octane-1-sulfonamide	MeFOSE	24448-09-7	8	Long chain
N-Ethylperfluorooctanesulfonamidoethanol	N-Ethyl-1,1,2,2,3,3,4,4,5,5,6,6,7,7,8,8-heptafluoro-N-(2-hydroxyethyl)octane-1-sulfonamide	EtFOSE	1691-99-2	8	Long chain
2-(Perfluorohexyl)ethanol	3,3,4,4,5,5,6,6,7,7,8,8-Tridecafluorooctan-1-ol	6 : 2 FTOH	647-42-7	8	Long chain
2-(Perfluorohexyl)ethyl acrylate	3,3,4,4,5,5,6,6,7,7,8,8-Tridecafluoroethyl prop-2-enoate	6 : 2 FTAC	17527-29-6	8	Long chain
2-(Perfluorohexyl)ethane-1-sulfonic acid	3,3,4,4,5,5,6,6,7,7,8,8-Tridecafluoroctane-1-sulfonic acid	6 : 2 FTSA	27619-97-2	8	Long chain
Mono[2-(perfluorohexyl)ethyl] phosphate	3,3,4,4,5,5,6,6,7,7,8,8-Tridecafluoroethyl dihydrogen phosphate	6 : 2 MonoPAP	57678-01-0	8	Long chain
Bis[2-(perfluorohexyl)ethyl] phosphate	bis(3,3,4,4,5,5,6,6,7,7,8,8-Tridecafluoroethyl) hydrogen phosphate	6 : 2 DiPAP	57677-95-9	8 <sup>a</sup>	Long chain
2-(Perfluorohexyl)ethyl methacrylate	3,3,4,4,5,5,6,6,7,7,8,8-Tridecafluoroethyl 2-methylprop-2-enoate	6 : 2 FTMAC	2144-53-8	8	Long chain
Perfluorononanoic acid	2,2,3,3,4,4,5,5,6,6,7,7,8,8,9,9-Heptafluorononanoic acid	PFNA	375-95-1	9	Long chain
Perfluorodecanoic acid	2,2,3,3,4,4,5,5,6,6,7,7,8,8,9,9,10,10-Nonadecafluorodecanoic acid	PFDA	335-76-2	10	Long chain
2-(Perfluorooctyl)ethanol	3,3,4,4,5,5,6,6,7,7,8,8,9,9,10,10-Heptafluorodecan-1-ol	8 : 2 FTOH	678-39-7	10	Long chain
2-(Perfluorooctyl)ethyl acrylate	3,3,4,4,5,5,6,6,7,7,8,8,9,9,10,10-Heptafluorodecyl prop-2-enoate	8 : 2 FTAC	27905-45-9	10	Long chain
Mono[2-(perfluorooctyl)ethyl] phosphate	3,3,4,4,5,5,6,6,7,7,8,8-Tridecafluoroethyl dihydrogen phosphate	8 : 2 MonoPAP	57678-03-2	10	Long chain
Bis[2-(perfluorooctyl)ethyl] phosphate	bis(3,3,4,4,5,5,6,6,7,7,8,8,9,9,10,10-Heptafluorodecyl) hydrogen phosphate	8 : 2 DiPAP	678-41-1	10	Long chain
2-(Perfluorooctyl)ethyl methacrylate	3,3,4,4,5,5,6,6,7,7,8,8,9,9,10,10-Heptafluorodecyl 2-methylprop-2-enoate	8 : 2 FTMAC	1996-88-9	10	Long chain
Perfluoroundecanoic acid	2,2,3,3,4,4,5,5,6,6,7,7,8,8,9,9,10,10,11,11-Henicosafluoroundecanoic acid	PFUnDA	2058-94-8	11	Long chain
Perfluorododecanoic acid	2,2,3,3,4,4,5,5,6,6,7,7,8,8,9,9,10,10,11,11,12,12,12-Tricosafuorododecanoic acid	PFDoDA	307-55-1	12	Long chain
2-(Perfluorodecyl)ethanol	3,3,4,4,5,5,6,6,7,7,8,8,9,9,10,10,11,11,12,12,12-Henicosafluorododecan-1-ol	10 : 2 FTOH	865-86-1	12	Long chain

Table 1 (Contd.)

Common name	IUPAC name	Acronym	CAS number	Carbon chain length	Classification
2-(Perfluorodecyl)ethyl acrylate	3,3,4,4,5,5,6,6,7,7,8,8,9,9,10,10,11,11,12,12,12-Henicosafuorodecyl prop-2-enoate	10 : 2 FTAC	17741-60-5	12	Long chain
2-(Perfluorodecyl)ethyl methacrylate	3,3,4,4,5,5,6,6,7,7,8,8,9,9,10,10,11,11,12,12,12-Henicosafuorodecyl 2-methylprop-2-enoate	10 : 2 FTMAC	2144-54-9	12	Long chain
Perfluorotridecanoic acid	2,2,3,3,4,4,5,5,6,6,7,7,8,8,9,9,10,10,11,11,12,12,13,13-Pentacosafuorotridecanoic acid	PFTrDA	72629-94-8	13	Long chain
Perfluorotetradecanoic acid	2,2,3,3,4,4,5,5,6,6,7,7,8,8,9,9,10,10,11,11,12,12,13,13,14,14-Heptacosafuorotetradecanoic acid	PFTeDA	376-06-7	14	Long chain
Perfluoropentadecanoic acid	2,2,3,3,4,4,5,5,6,6,7,7,8,8,9,9,10,10,11,11,12,12,13,13,14,14,15,15-Nonacosafuoropentadecanoic acid	PFPeDA	141074-63-7	15	Long chain

<sup>a</sup> On each side.

(LC) and short-chain (SC) compounds, which contain at least eight and fewer than eight carbon atoms, respectively.<sup>6</sup> However, the OECD provides a more detailed categorization, defining long-chain PFAS as perfluoroalkyl carboxylic acids (PFCAs) with more than seven carbons, perfluoroalkyl sulfonic acids (PFSAs) with more than six carbons, and substances that can degrade into long-chain PFCAs and PFSAs,<sup>7</sup> such as perfluorooctanoic acid (PFOA) and perfluorooctane sulfonate (PFOS).

While PFOA and PFOS are the most recognized long-chain PFAS, the broader category includes other compounds like perfluorononanoic acid (PFNA) and perfluorodecanoic acid (PFDA), which also possess persistent properties that make them physiologically harmful.<sup>8</sup> Other long-chain PFCAs include perfluoroundecanoic acid (PFUnDA), perfluorododecanoic acid (PFDoDA), perfluorotridecanoic acid (PFTrDA), perfluorotetradecanoic acid (PFTeDA), and perfluoropentadecanoic acid (PFPeDA).<sup>9</sup> Moreover, some PFCA precursors include fluorotelomer alcohols (FTOHs),<sup>10</sup> fluorotelomer acrylates (FTACs)<sup>10</sup> and methacrylates (FTMs),<sup>10</sup> fluorotelomer sulfonates (FTSAs)<sup>11</sup> and polyfluoroalkyl phosphate esters (PAPs and diPAPs).<sup>11</sup> Additionally, some perfluoroalkane sulfonamides (PFASAs), precursors for PFSAs, were detected in environmental and biological matrices, including perfluorooctanesulfonamide (PFOSA), *N*-methylperfluorooctanesulfonamide (MeFOSA), *N*-ethylperfluorooctanesulfonamide (EtFOSA), *N*-methylperfluorooctanesulfonamidoethanol (MeFOSE), *N*-ethylperfluorooctanesulfonamidoethanol (EtFOSE).<sup>12</sup> Perfluorohexanoic acid (PFHxA) and perfluorohexanesulfonic acid (PFHxS) have also been heavily discussed in the literature due to their serious toxicological effects.<sup>13</sup>

Short-chain PFAS usually refer to compounds containing between four and six carbon atoms, while ultrashort-chain PFAS include those with one and three carbon atoms.<sup>14</sup> Short-chain and ultrashort-chain PFAS molecules have been poorly studied in the literature due to multiple challenges. Those challenges encompass their limited scope of analysis due to their high polarity and the perception that they are less harmful, less persistent, and less accumulative than their long-chain counterparts.<sup>14</sup> However, some studies have shown that exposure to short and ultrashort-chain PFAS appears to have multiple adverse effects on reproductive, developmental, hepatic, and renal health.<sup>15-17</sup> Moreover, short-chain PFAS have historically received less regulatory attention compared to the longer chain ones.<sup>14</sup> In general terms, short-chain PFAS include perfluorobutanoic acid (PFBA), perfluoropentanoic acid (PFPeA), perfluorobutanesulfonic acid (PFBS), and perfluoropentanesulfonic acid (PFPeS), whereas ultrashort-chain PFAS include trifluoroacetic acid (TFA), perfluoropropanoic acid (PFPrA) and perfluoropropanesulfonic acid (PFPrS).<sup>18</sup> The global fate and transport of ultrashort- and short-chain PFAS remain poorly understood, with two main hypotheses proposed in the literature regarding their movement in the environment.<sup>14</sup> The first hypothesis proposes that marine aerosols are the primary mode of transport of ionic PFAS,<sup>19</sup> whereas the second hypothesis suggests that volatile



PFAS precursors are transported to remote regions and contaminate the environment with short-chain PFAS through degradation mechanisms.<sup>20</sup>

PFAS are synthetic chemical substances extensively employed since the mid-20th century in a wide variety of industrial processes and consumer products due to their physicochemical properties, including exceptional stability, hydrophobicity, lipophobicity, and heat resistance. The widespread use of PFAS stems primarily from their role as critical components in surfactants, lubricants, water- and stain-repellent coatings, and fire-fighting foams. Major industrial sources include primary manufacturing facilities, where a wide variety of PFAS are released into the environment. For example, fluoropolymer manufacturing plants emit PFAS, such as multi-head perfluoroalkyl ether sulfonates (PFESs), into the air, soil, and water. Studies have shown that both gas-phase and particle-phase PFAS are present in high concentrations inside and outside FMEs. These emissions can travel significant distances, especially short-chain PFAS, which are particularly mobile.<sup>21,22</sup>

Once airborne, PFAS can exist in both gas and particle-bound forms. Neutral compounds such as FTOHs and PFOSAs are found in higher concentrations in the atmosphere than ionic PFAS.<sup>23</sup> Wastewater treatment plants (WWTP) have also been shown to be critical PFAS sources in the atmosphere throughout various mechanisms, particularly PFAS present in water can volatilize during aeration and other possible treatments, as air samples collected over WWTP showed high levels of FTOHs and conversely low concentrations of PFOSAs derivatives.<sup>24,25</sup> PFAS were also detected in regions where all of the previous sources are not present, indicating long-range atmospheric transport (LRAT), where PFAS molecules travel long distances in the atmosphere.<sup>26</sup> In brief, the widespread and persistent presence of PFAS in the atmosphere results from several overlapping emission sources, ranging from industrial manufacturing and wastewater treatment plants as the major contributors, to consumer product usage and degradation. Their chemical stability and volatility, particularly for neutral PFAS such as FTOHs and PFOSAs, permit them to persist in the environment and be transported to remote ecosystems such as the Amazon and the Arctic. Moreover, textile and metal coating sites incorporate PFAS into products such as textiles, leather, carpets, paper, and cardboard. This leads to contamination of air, soil, and sediment through emissions, spills, and improper waste disposal. When polyamide fabrics are exposed to natural elements such as sunlight, precipitation, and wind, distinct patterns of perfluoroalkyl acids (PFAAs) were emitted from each side-chain fluorinated polymer textile used to coat materials to make them water-repellent. PFAS can also migrate from the inner to the outer layers of multilayered fabrics, leading to environmental release through surface contact and washing.<sup>27,28</sup>

Firefighting foam, particularly aqueous film-forming foams (AFFF), has historically been a significant source of PFAS contamination.<sup>29</sup> Consumer products are considered another pervasive source. For example, PFAS have been found in stain-resistant carpeting and nonstick cookware.<sup>30</sup> Moreover, several studies have detected significant levels of PFAS in cosmetic products, including cyclic perfluorinated alkanes,

perfluorinated ethers, and polyfluorinated silanes.<sup>31</sup> In this case, PFAS release occurs during production, handling, and waste management.

PFAS have been widely used in industrial and consumer products since the 1940's. However, they pose significant risks to human health due to their persistence in the environment, potential for bioaccumulation, and diverse toxicological effects.<sup>32–34</sup> These “forever chemicals” are linked to a range of adverse health outcomes. Among their most documented effects are disruption to lipid metabolism, thyroid dysfunction, immune suppression, and developmental disruption.<sup>32–34</sup>

PFAS, especially PFOA and PFOS, have been shown to disrupt thyroid homeostasis through multiple mechanisms. These molecules inhibit NIS-mediated iodide uptake into thyroid follicular cells, impairing thyroid function.<sup>34</sup> PFOS tends to mimic the effect of the NIS inhibitor perchlorate in its ability to prevent iodide uptake, disrupting hormonal balance.<sup>34</sup> Studies found that higher PFOA, PFUnDA, PFOS,  $\sum_4$  PFAS (PFOA + PFOS + PFNA + PFHxS), and  $\sum_{LC}$  PFAS concentrations were associated with a slight increase in free T4 in teenage boys, suggesting that environmentally relevant concentrations of PFAS may be associated with subtle alterations in the thyroid hormone.<sup>35</sup> Nonetheless, other studies suggested that in both female and male adolescents, higher PFOA and PFAS concentrations were associated with lower T4 and lower levels of the Thyroid Stimulating Hormone.<sup>36</sup> Though PFAS can induce both hypothyroid and hyperthyroid effects, both outcomes confirm its disruptive impact on the thyroid gland.

PFAS exposure has been consistently associated with impaired immunity and reduced vaccine response in young children.<sup>37</sup> Epidemiological research shows that elevated PFAS levels correlate with reduced antibody production following vaccinations, particularly in children.<sup>37</sup> In adolescents, while antibody levels naturally decline post-vaccination, PFAS exposure, particularly PFOS, accelerates this decline. However, tetanus antibody levels showed weaker associations, suggesting PFAS may selectively impair responses to certain vaccines. These results reinforce the conclusion that postnatal PFAS exposure drives immune suppression.<sup>38</sup>

PFAS have been proven to interfere with lipid homeostasis. For instance, a study of 753 middle aged Danes found significant positive correlations between plasma levels of PFOA, PFOS and total cholesterol levels, with a 4.4 mg dL<sup>-1</sup> increase in cholesterol per interquartile range rise in PFOA exposure. Similar trends could also be observable with adolescents, as PFOS exposure was linked to 53% higher chances of elevated low-density lipoproteins (LDL).<sup>32</sup> These results align with another cohort of the same line in Sweden, where positive correlations were found between PFOA, PFOS, PFDA, and an increase in cholesterol levels.<sup>39</sup> A possible mechanism to explain it could be that PFAS alters gene expression in liver cells, as a study found that PFAS-associated DNA methylation in genes like USF2 and CREB5 mediated up to 47% of the observed increase in LDL cholesterol.<sup>40</sup>

The International Agency for Research on Cancer (IARC) classifies PFAS as a carcinogen, with PFOA classified as a human carcinogen (Group 1) and PFOS classified as a potential



carcinogen (Group 2B).<sup>41</sup> Additionally, studies conducted in the United States associated PFOA exposure with renal cell carcinoma formation, exclusively among women. Among men, a positive association was observed between PFHxS concentration and chronic lymphatic leukaemia.<sup>42</sup> Moreover, epidemiological research has identified an association between PFAS exposure and an increased risk of cancer, particularly kidney and testicular cancer.<sup>43</sup> Nonetheless, these associations remain limited to certain types of cancer. It is essential to understand the mechanistic pathways through which PFAS can impact cancer risks in individuals. One proposed mechanism is the induction of oxidative stress, in which PFAS exposure has been shown to increase the cell's production of reactive oxygen species (ROS), which can lead to damage to cellular components, including DNA.<sup>44</sup> This damage can result in several mutations, which promote carcinogenesis. In a study conducted by Obiako *et al.* (2024), cells exposed to PFOA and PFBA produced significantly more ROS compared to untreated cells.<sup>44</sup> Another mechanism involves epigenetic effects of PFAS on the cell; in several studies, positive correlations were made between epigenetic age, DNA methylation, and PFAS exposure.<sup>45</sup> Data indicate that firefighters, a population that is the most exposed to PFAS, showed DNA methylation at a specific DNA sequence and accelerated aging patterns.<sup>45</sup>

Overall, although the toxicological literature clearly demonstrates risks, a complete understanding of population exposure requires tracing PFAS emissions through the atmosphere, where their persistence and mobility link industrial sources to remote receptors, including humans. Although PFAS toxicology and sources are increasingly well characterized, their atmospheric behavior remains less well understood. Bridging this knowledge gap is critical, as atmospheric transport and

deposition are the primary routes by which PFAS reach remote ecosystems and contribute to long-term exposure risks. Therefore, this review synthesizes current research on atmospheric PFAS by focusing on three key areas: (1) their levels and distribution across polar, midlatitude, and tropical regions; (2) the role and mechanisms of wet deposition, *via* snowfall, rainfall, ice, and surface water, in determining their atmospheric fate; and (3) their chemical transformations and phase partitioning behavior in the atmosphere.

## 2. Comparison of the levels of PFAS in the global atmosphere across several regions

In this review, we define polar regions as those located north of 66.5°N latitude (Arctic Circle), and south of 66.5°S latitude (Antarctic Circle), and subpolar regions as roughly between 55°N/S and 66.5°N/S (Fig. 1), characterized by extreme seasonal variations in solar radiation, persistent cold temperatures, and unique atmospheric conditions.<sup>47</sup>

### 2.1. Polar and subpolar regions

Neutral PFAS, including FTOHs, PFOSA derivatives and perfluorooctanesulfonamidoethanols (FOSEs), are persistent pollutants that undergo long-range atmospheric transport (LRAT) to remote regions, such as polar and subpolar zones. Literature has documented their occurrence in Arctic, Antarctic, and open oceans, with predominance in the gas phase due to their increased volatility. For example, in a study investigating the occurrence of PFAS along an extensive Arctic route, the gas-phase concentrations detected showed mean levels of FTOHs in

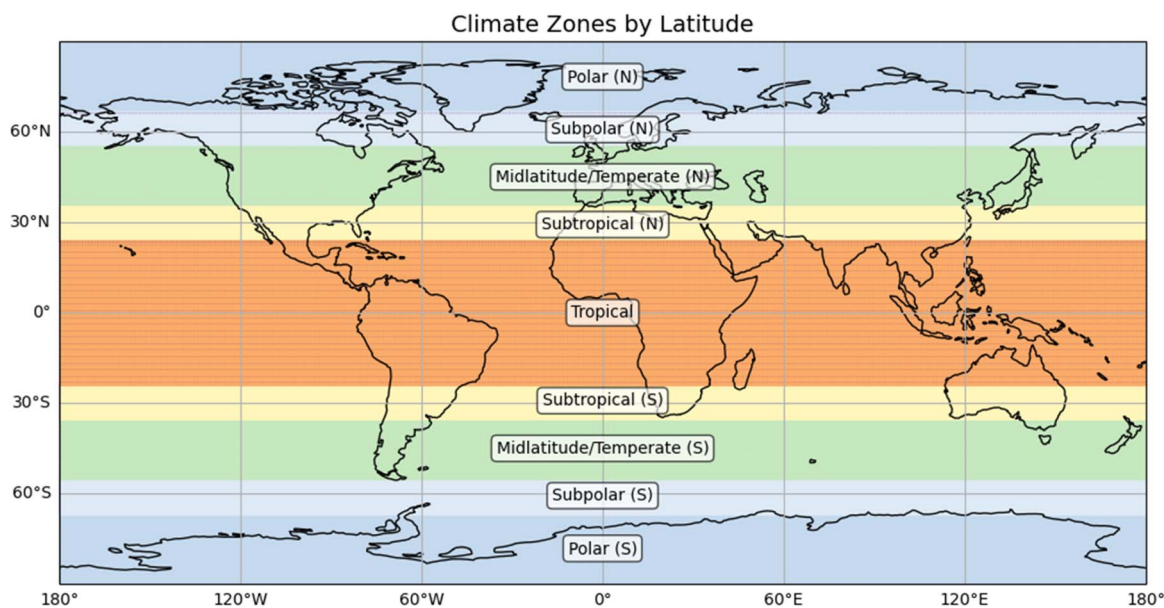


Fig. 1 Classification of climate zones by latitude. Polar regions are located north of 66.5°N latitude (Arctic Circle), and south of 66.5°S latitude (Antarctic Circle), and subpolar regions roughly between 55°N/S and 66.5°N/S. The midlatitude and temperate zone includes regions roughly from 35° to 55° latitude in both hemispheres. Tropical regions are localized between the Tropics of Cancer from 23.5°N and 23.5°S, while subtropical regions are localized between approximately 23.5° and 35° latitude in both hemispheres, bordering the tropics.



the following trend: 8 : 2 FTOH ( $11.4 \text{ pg m}^{-3}$ ) > 10 : 2 FTOH ( $6.27 \text{ pg m}^{-3}$ ) > 6 : 2 FTOH ( $2.65 \text{ pg m}^{-3}$ ).<sup>46</sup> The methodology of air sampling appears to be consistent among various studies. Glass fiber filters (GFFs) are used for particle-phase sampling, while polyurethane foam/XAD-2 cartridges are used for gas-phase PFAS collection.<sup>48–50</sup> The analytical tool used in studying volatile PFAS is gas chromatography mass spectrometry with positive chemical ionization in selective ion monitoring mode. The standardization of techniques among various studies allows direct comparison of PFAS levels across polar and subpolar regions.

Across latitudes approximately between  $55.7^\circ\text{S}$  and  $70.4^\circ\text{S}$ , and longitudes from just east of the Prime Meridian ( $0.001^\circ\text{E}$ ) to  $73.2^\circ\text{W}$  (blue box shown in Fig. 2), the average concentration of 8 : 2 FTOH ( $22.04 \text{ pg m}^{-3}$ ) was significantly higher than that of 10 : 2 FTOH ( $3.67 \text{ pg m}^{-3}$ ), which in turn exceeded the level of 6 : 2 FTOH ( $0.65 \text{ pg m}^{-3}$ ).<sup>48</sup> However, in the western Antarctic Peninsula, approximately  $54\text{--}69^\circ\text{S}$  and  $60\text{--}75^\circ\text{W}$  (green box shown in Fig. 2), lower levels of FTOHs were detected, but with a similar trend: 8 : 2 FTOH ( $6 \text{ pg m}^{-3}$ ) > 10 : 2 FTOH ( $2.7 \text{ pg m}^{-3}$ ) > 6 : 2 FTOH ( $1.2 \text{ pg m}^{-3}$ ).<sup>50</sup> On one hand, the former includes regions that could be closer to industrial areas, major shipping routes, and continental outflow from South America and Africa.<sup>48</sup> On the other hand, the Western Antarctic Peninsula is a more localized and limited zone, with a strong indication of atmospheric transport and degradation processes.<sup>50</sup> In regard to the levels of FOSEs and PFOSA derivatives, they appear to be comparable in the two zones and low with the following trend: MeFOSE > MeFOSA > EtFOSE  $\sim$  EtFOSA. It is important to indicate that data on PFAS concentrations in the Antarctic Peninsula remains scarce, and further work is necessary to understand the long-term distribution of forever chemicals and assess ecological risk.

The Canadian Arctic is a critical region for studying the levels of neutral PFAS in the atmosphere as it reflects LRAT patterns and PFAS distribution globally. The Canadian Arctic also plays a major role in underscoring early indicators for global contamination trends and the effectiveness of international environmental regulations. The occurrence of PFAS in such

pristine environments is mainly driven by transport processes due to their chemical persistence.<sup>51</sup> Comparing the levels of FTOHs among Hudson Bay (Fig. 3A), Beaufort Sea (Fig. 3B), and Labrador Sea (Fig. 3C), the levels of 8 : 2 FTOH are higher than those of 10 : 2 FTOH and 6 : 2 FTOH. As depicted in Fig. 3, the level of 8 : 2 FTOH is slightly higher in Hudson Bay ( $49 \text{ pg m}^{-3}$ ) than Beaufort Sea ( $44 \text{ pg m}^{-3}$ ) and Labrador Sea ( $40 \text{ pg m}^{-3}$ ).<sup>20</sup> For 10 : 2 FTOH, the levels are similar among the three locations, with concentrations of  $17 \text{ pg m}^{-3}$  in the Labrador Sea,  $14 \text{ pg m}^{-3}$  in Hudson Bay, and  $16 \text{ pg m}^{-3}$  in the Beaufort Sea.<sup>20</sup> The level of 6 : 2 FTOH is the highest in Hudson Bay ( $12 \text{ pg m}^{-3}$ ) and lowest in Labrador Sea ( $3.7 \text{ pg m}^{-3}$ ), while the level in Beaufort Bay was intermediate at  $9.3 \text{ pg m}^{-3}$ .<sup>20</sup> In another study conducted by Cai *et al.*,<sup>52</sup> the level of 8 : 2 FTOH in Beaufort Sea (Fig. 3D) ( $72.27^\circ\text{N}$ ,  $-153.28^\circ\text{E}$ ) was found to be higher than the former study<sup>20</sup> at  $82 \text{ pg m}^{-3}$ , but that of 6 : 2 FTOH and 10 : 2 FTOH were lower at  $1.7 \text{ pg m}^{-3}$  and  $13 \text{ pg m}^{-3}$ , respectively. However, the concentrations followed the same trend in both studies: 8 : 2 FTOH > 10 : 2 FTOH > 6 : 2 FTOH.<sup>20,52</sup> The differences observed could be attributed to the extraction protocol employed, sampling altitude, spatial coverage, and temporal variability. For instance, the two studies were conducted two years apart in terms of sampling dates. This time difference could have led to variations in environmental conditions such as temperature and atmospheric transport.

Moreover, Stock *et al.* revealed that the mean levels of FTOH in Cornwallis Island, approximately at  $74^\circ49'\text{N}$ ,  $94^\circ32'\text{W}$ , in the summer of 2004 were  $14 \text{ pg m}^{-3}$  (Fig. 3E),  $8.16 \text{ pg m}^{-3}$ , and  $2.8 \text{ pg m}^{-3}$  for 8 : 2 FTOH, 6 : 2 FTOH, 10 : 2 FTOH, respectively.<sup>26</sup> Interestingly, the levels of MeFOSE and EtFOSE appeared to be significantly higher than those of FTOHs at  $29 \text{ pg m}^{-3}$  and  $23 \text{ pg m}^{-3}$ , respectively.<sup>26</sup> This finding could be explained by referring to the increased usage of FOSEs in the early 2000s in various consumer products, including surface treatments and fire-fighting foams.<sup>55</sup> Genualdi *et al.* utilized passive air sampling to study the occurrence of PFAS at various locations, including two major sites in the Canadian Arctic: Alert ( $82.45^\circ\text{N}$ ,  $63.50^\circ\text{W}$ ) and Little Fox Lake ( $61.35^\circ\text{N}$ ,  $135.60^\circ\text{W}$ ).<sup>54</sup> The levels of 10 : 2 FTOH and 6 : 2 FTOH were below the limit of quantification (LOQ).<sup>54</sup>



Fig. 2 Atmospheric concentrations of FTOHs in Antarctica, as reported in prior studies.<sup>48,50</sup> The diameters of the circles are proportional to the detected concentrations.





Fig. 3 Atmospheric concentrations of 8 : 2 FTOH ( $\text{pg m}^{-3}$ ) in the Arctic, as reported in prior studies.<sup>20,26,49,52–54</sup> Measurements in the following locations are reported: (A) Hudson Bay, (B and D) Beaufort Sea, (C) Labrador Sea, (E) Cornwallis Island, (F) Canadian Arctic Alert, (G) Little Fox Lake, (H) High Arctic Ocean, (I) Chukchi Sea, (J) Bering Sea, (K) Ny-Ålesund, (L) Villum Research Station.

For 8 : 2 FTOH, concentrations were  $6.41 \text{ pg m}^{-3}$  in Alert and  $16.1 \text{ pg m}^{-3}$  in Little Fox Lake, identified in Fig. 3 as points F and G, respectively.<sup>54</sup> The levels of FOSEs and PFOSA derivatives were below the LOQ in both locations. Such low levels of 10 : 2 FTOH, 6 : 2 FTOH, FOSEs and PFOSA derivatives might reflect lower atmospheric prevalence in the studied region, whereas the elevated levels of 8 : 2 FTOH could reveal its common use and greater environmental persistence. Further research is critical to study and analyze PFAS contamination in the Canadian Arctic, with emphasis on identifying emission sources and transport pathways. Expanding analytical datasets in this region would be significant to understand the LRAT of neutral PFAS and their presence in polar ecosystems.

Furthermore, elevated levels of neutral PFAS were revealed along the northward trajectory through the Arctic.<sup>52</sup> Referring to Fig. 3 points H, I, and J, the levels of 8 : 2 FTOH were the highest in the high Arctic Ocean ( $81.5^\circ\text{N}$ ,  $-167.14^\circ\text{E}$ ), followed by Chukchi Sea ( $66.43^\circ\text{N}$ ,  $-168.81^\circ\text{E}$ ), and Bering Sea ( $62.64^\circ\text{N}$ ,  $-175.12^\circ\text{E}$ ) at  $160 \text{ pg m}^{-3}$ ,  $124 \text{ pg m}^{-3}$ , and  $103 \text{ pg m}^{-3}$ , respectively.<sup>52</sup> The concentrations of 10 : 2 FTOH followed the same trend as that of 8 : 2 FTOH at  $31 \text{ pg m}^{-3}$ ,  $18 \text{ pg m}^{-3}$ , and  $11 \text{ pg m}^{-3}$ , respectively.<sup>52</sup> Those levels could be explained by the global distillation phenomenon, where PFAS migrate from warmer regions poleward to colder ones.<sup>56</sup> FTOHs are volatile compounds that could be transported over long distances prior to their condensation or deposition. As for the levels of FOSEs, the levels of MeFOSE and EtFOSE in the high Arctic Ocean were  $0.4 \text{ pg m}^{-3}$  and  $0.7 \text{ pg m}^{-3}$ , respectively.<sup>52</sup> However, those levels were the same in both the Chukchi Sea and the Bering Sea at  $0.1 \text{ pg m}^{-3}$ .<sup>52</sup> Generally, the levels of FOSEs are lower than those of FTOHs due to shorter atmospheric lifetimes and degradation en route, limiting their prevalence in the Arctic atmosphere.

It appears that the levels of PFAS between the Eastern Arctic and Western Arctic differ. The classification for the Eastern

Arctic and Western Arctic is based on the Primephase Meridian ( $0^\circ$ ), where the regions to the east of the Prime Meridian are considered the former and those to the west are referred to as the latter. In one of the research stations in the Eastern Arctic, in Ny-Ålesund ( $78^\circ55'\text{N}$ ,  $11^\circ56'\text{E}$ ), the concentration of 8 : 2 FTOH ( $10 \text{ pg m}^{-3}$ ; Fig. 3K) is roughly five times that of 10 : 2 FTOH and 6 : 2 FTOH.<sup>49</sup> However, the levels of MeFOSE, MeFOSA, EtFOSE, and EtFOSA show<sup>49</sup> slight variations, with the highest level for MeFOSA at  $0.3 \text{ pg m}^{-3}$  and the lowest for EtFOSE at  $0.1 \text{ pg m}^{-3}$ . In the Western Arctic, at Villum Research Station, Station Nord ( $81^\circ36'\text{N}$ ,  $16^\circ40'\text{W}$ ), the concentration of 8 : 2 FTOH ( $4.9 \text{ pg m}^{-3}$ ; Fig. 3L) is roughly half of that in Ny-Ålesund, while that of 10 : 2 FTOH and 6 : 2 FTOH are comparable.<sup>53</sup> However, the concentrations of FOSEs and PFOSA derivatives in the Villum Research station<sup>53</sup> are slightly higher than those of Ny-Ålesund.<sup>49</sup> The results of comparisons could be attributed to the greater proximity of Ny-Ålesund to European industrial regions and seasonal melt, which is less prevalent at Villum Research Station, Station Nord, where direct input is minimal and ice is more locked.

Neutral PFAS are prevalent in the Arctic, Antarctic and subpolar regions, primarily in the gas phase, with varying levels across multiple regions. The concentration trend of FTOH seems to be consistent with 8 : 2 FTOH > 10 : 2 FTOH > 6 : 2 FTOH. It holds true across various locations, such as the Arctic route, the Western Antarctic Peninsula, the Canadian Arctic, and the High Arctic Ocean. Elevated levels of FTOH are generally observed in zones close to industrialized regions and transportation routes. The concentrations of MeFOSE and MeFOSA are generally low, likely due to their shorter atmospheric lifetimes and degradation patterns; however, some studies report higher levels, reflecting their past widespread use. The literature covering the distribution of PFAS in the polar regions remains limited and underdeveloped, particularly in



the Antarctic Peninsula. Further studies should be conducted to enhance the regional understanding of PFAS in such pristine environments to better assess their sources, transport pathways, and environmental fate.

## 2.2. Midlatitude and temperate regions

Midlatitude and temperate regions, spanning roughly from 35° to 55° latitude in both hemispheres, serve as a transitional zone between the subtropics and polar areas<sup>57</sup> (Fig. 1). These regions are characterized by major seasonal variability, with four distinct seasons and climates ranging from oceanic, milder and wetter, to continental, drier and with greater temperature fluctuations.<sup>58</sup> Due to the interplay of warm and cold air masses, midlatitude weather is highly dynamic and variable.<sup>58</sup> Importantly, these areas encompass many of the world's industrialized zones, particularly across North America, Europe, and East Asia, where the majority of PFAS production and application have historically occurred.<sup>59</sup> Not only do midlatitudes function as primary emission sources but also as key atmospheric and hydrological transport pathways for PFAS, facilitating their transport toward more pristine environments like the Arctic. Additionally, the midlatitudes encompass not only industrialized regions but also remote ones, portraying diverse atmospheric conditions. This could be exemplified by locations such as the Tibetan Plateau and Mace Head that exhibit PFAS occurrence, with 8 : 2 FTOH levels reaching 30 pg m<sup>-3</sup> in Muztagata in the Tibetan Plateau (38.27°N, 74.85°E)<sup>60</sup> and 11.3 pg m<sup>-3</sup> in Mace Head (53.17°N, 9.50°W; Fig. 6 point J).<sup>61</sup>

The Northwest Pacific and Japanese Marginal Seas are considered coastal and marginal seas of East Asia, including areas off China, Japan and Korea. The area is heavily influenced by the Kuroshio Current, a warm western boundary ocean current that affects the distribution of pollutants, atmospheric

deposition, and the composition of air masses.<sup>62</sup> This zone also exhibits a combination of clean marine air and transboundary pollution outflow events from industrialized regions.<sup>63</sup> The area represents a wide spatial range from background environments to more impacted ones. In the Sea of Japan, near East China Sea and Korea Strait, roughly placed at coordinates of 36.55°N and 131.97°E, the levels of FTOHs, prevalent in the gas phase, are significant with 250 pg m<sup>-3</sup> for 8 : 2 FTOH (Fig. 4A) and a total concentration of 13 PFAS at 346 pg m<sup>-3</sup>. The levels of MeFOSE, MeFOSA, EtFOSE, and EtFOSA are low at 0.2 pg m<sup>-3</sup>, with the exception of EtFOSA at 0.5 pg m<sup>-3</sup>.<sup>52</sup> At coordinates of roughly 45.09°N, 140.30°E, off coast of Hokkaido, Japan's northernmost main island, the levels of FTOHs are slightly higher with 8 : 2 FTOH at 289 pg m<sup>-3</sup> (Fig. 4B), whereas the levels of FOSEs and PFOSA derivatives are roughly the same. The total concentration of PFAS is 416 pg m<sup>-3</sup>.<sup>52</sup> A possible oceanographic explanation for the observed gas-phase FTOH concentrations is the influence of ocean currents on air-sea exchange and atmospheric chemistry. The Sea of Japan near Korea Strait is greatly influenced by ocean currents and exchange with East China Sea and Pacific Ocean,<sup>64</sup> which could possibly dilute or rapidly disperse FTOHs. However, off the coast of Hokkaido, the region is affected by the colder Oyashio Current,<sup>65</sup> enhancing accumulation and reducing the rate of oxidation into other forms.

Furthermore, the levels of PFAS tend to vary notably across different marine regions in East Asia, with samples collected near eastern Taiwan, southern Japan's Ryukyu Islands, northern Japan's Tohoku region, and northern Honshu close to the Sea of Japan.<sup>67</sup> Specifically, the highest level of 8 : 2 FTOH is 170 pg m<sup>-3</sup> in southern Japan's Ryukyu Island, while the lowest is 12 pg m<sup>-3</sup> in northern Japan's Tohoku region.<sup>67</sup> This could be attributed to the influence of the Ryukyu Islands to subtropical westerlies and monsoonal flows,<sup>68</sup> facilitating the transport of FTOHs from point sources, as well as its proximity to



Fig. 4 Atmospheric concentrations of 8 : 2 FTOH (pg m<sup>-3</sup>) in selected regions in Asia, as reported in prior studies.<sup>25,52,66</sup> Measurements in the following locations are reported: (A) Sea of Japan, (B) off coast of Hokkaido, (C) Tianjin, (D) Beijing.





Fig. 5 Concentrations of ionic PFAS (PFOA & PFOS) in the particulate phase sampled from both Northern Honshu, Sea of Japan and Near Eastern Taiwan, as reported in prior work.<sup>67</sup>

industrialized zones in southern China, Taiwan, and southern Japan.<sup>69</sup> According to Fig. 5, in regard to the levels of ionic PFAS, predominantly in the particulate phase, the levels of PFOA and PFOS are the greatest in northern Honshu close to the Sea of Japan,  $43 \text{ pg m}^{-3}$  and  $5.2 \text{ pg m}^{-3}$ , respectively, and lowest near eastern Taiwan,  $3.5 \text{ pg m}^{-3}$  and  $1.1 \text{ pg m}^{-3}$ , respectively.<sup>67</sup> Those findings are particularly attributed to the former region receiving continental air masses with higher ambient particulate matter levels, promoting PFAS adsorption onto the particles. The levels of shorter chain PFAS, such as PFHxS and PFHxA, are lower and show less variability than their longer counterparts.<sup>67</sup> For instance, the levels of PFHxS are similar at  $1.5 \text{ pg m}^{-3}$  near eastern Taiwan, southern Japan's Ryukyu Islands, and northern Japan's Tohoku region, but slightly higher in northern Honshu close to the Sea of Japan at  $2.5 \text{ pg m}^{-3}$ .

Moreover, the East Asian continental belt is a zone characterized by high population density and heavy industrialization stretching across eastern China, the Korean Peninsula and regions in Japan.<sup>70</sup> Remarkably, this zone encompasses the world's largest megacities, such as Seoul and Tokyo, making it a major hub for extensive industrial and manufacturing activities.<sup>70</sup> It is also characterized by rapid economic development and urbanization,<sup>70</sup> increasing the levels of atmospheric pollutants.<sup>71</sup> The region has been affected by the global shift in

fluorochemical production, where it has increasingly moved from Western countries to East Asia,<sup>72</sup> mainly due to lower labor costs, fewer regulatory restrictions, and increased local demand. A study assessed the levels of PFAS across urban locations in Korea using a passive air sampler (PAS) with polyurethane foam (PUF) and sorbent-impregnated polyurethane foam (SIP), commonly used to collect airborne PFAS for environmental monitoring with a sorbent to enhance the capture of such compounds and without active pumping.<sup>73</sup> The average concentrations from 6 urban samples of 10:2 FTOH, 8:2 FTOH, MeFOSE, and MeFOSA were  $10125 \text{ pg m}^{-3}$ ,  $9346 \text{ pg m}^{-3}$ ,  $113 \text{ pg m}^{-3}$ ,  $121 \text{ pg m}^{-3}$ , respectively, reflecting the prevalence of emissions from point sources.<sup>73</sup> Using XAD-PAS, which is not capable of distinguishing between gas-phase and particulate-phase PFAS, the levels of PFAAs and PFSAs were analyzed across urban and rural locations, mostly covering the Eastern China region.<sup>74</sup> The mean levels showed the following trend:  $\text{PFOA} > \text{PFHxA} > \text{PFOS} > \text{PFNA} > \text{PFUnDA} > \text{PFHxS}$ .<sup>74</sup> This trend could be attributed to the historical use of PFOA and PFHxA in China for manufacturing textiles, coatings, and firefighter foams, whereas longer-chain PFAA, such as PFNA and PFUnDA, are less extensively produced.<sup>75</sup> The lower levels of PFOS reflect its legacy contamination and restricted use in industrial applications,<sup>75</sup> as it was one of the first PFAS to be regulated under the Stockholm Convention.<sup>76</sup>



Tianjin is a major industrial and coastal city in northeastern China, known for petrochemical and fluorochemical industries.<sup>77</sup> Yao *et al.* examined the levels of PFAS in Tianjin during both Summers of 2013 (ref. 25) and 2014 (ref. 78) using passive air sampling with PUF-SIP<sup>25</sup> and active air sampling with PUF/XAD and GFFs,<sup>78</sup> respectively. In regard to the levels of FTOHs, they followed the same trend in both studies: 8 : 2 FTOH > 10 : 2 FTOH > 6 : 2 FTOH,<sup>25,78</sup> but such concentrations were higher in the 2014 (ref. 78) than 2013.<sup>25</sup> For instance, the concentrations of 8 : 2 FTOH in 2014 ( $225 \text{ pg m}^{-3}$ )<sup>78</sup> were roughly 2.8 times higher than those in 2013 ( $81.7 \text{ pg m}^{-3}$ ; Fig. 4C).<sup>25</sup> This could possibly be attributed to increased fluoropolymer production and short-term spikes that are smoothed out in PAS. Regarding the levels of PFOS, they were significantly higher in sampling campaign of Summer 2014 ( $470 \text{ pg m}^{-3}$ )<sup>78</sup> as compared to that of Summer 2013 ( $3.4 \text{ pg m}^{-3}$ ),<sup>25</sup> possibly due to the unauthorized use of PFOS in fluoropolymer production or underrepresentation by PAS. However, the concentrations of PFOA didn't exhibit a significant difference across the two studies.<sup>25,78</sup>

In Fuxin, China, near a fluorochemicals point source, the level of PFBA was significantly high reaching  $1100 \text{ pg m}^{-3}$ , followed by PFOA at  $600 \text{ pg m}^{-3}$ .<sup>79</sup> In Beijing, the capital city of China, the concentrations of various PFAS were reported, where the concentrations of 8 : 2 FTOH, 6 : 2 FTOH, 10 : 2 FTOH, and PFBA were significant at  $177.2 \text{ pg m}^{-3}$  (Fig. 4D),  $26.6 \text{ pg m}^{-3}$ ,  $43.2 \text{ pg m}^{-3}$ , and  $44.7 \text{ pg m}^{-3}$ , respectively.<sup>66</sup> Other PFASs were detected at low concentrations such as PFHxA and PFNA at  $1.3 \text{ pg m}^{-3}$  and  $1.1 \text{ pg m}^{-3}$ , respectively.<sup>66</sup> Those two studies exhibit a distinction between point-source emissions<sup>79</sup> and regional or cumulative pollution.<sup>66</sup> The contrast highlights the spatial

heterogeneity of PFAS emissions, where proximity to a dominant point source could lead to locally elevated levels. The wide distribution of neutral and ionic PFAS across the East Asian continental belt underscores the need to expand regional atmospheric analysis of these compounds. Such regions could act as hotspots for PFAS accumulation and drivers of their atmospheric transport to more remote atmospheres, affecting global PFAS dispersion.

The North Sea, including its southeastern extension known as the German Bight, is a heavily industrialized and anthropogenically influenced region in northwestern Europe.<sup>80</sup> The region also experiences dynamic air-sea interactions due to the occurrence of high winds, cyclonic activity and efficient land-mass sea exchanges.<sup>81</sup> The North Sea and its coastal zones have been historically renowned for their petrochemical industries, offshore gas extractions, and shipping activities. Through a cruise sampling campaign from Bremerhaven, a port city on the coast of the North Sea, to the Bay of Biscay, elevated levels of FTOHs were detected, reflecting regional contamination.<sup>82</sup> Notably, coastal zones exhibit higher levels of FTOHs *via* input from nearby sources.<sup>83</sup> For instance, as shown in Fig. 6 points A, B, and C respectively, the concentrations of 8 : 2 FTOH in the German Bight, near Heligoland ( $56 \text{ pg m}^{-3}$ ), and the West Frisian coast ( $28 \text{ pg m}^{-3}$ ) are higher than that in the Dutch Exclusive Economic Zone, an offshore marine environment ( $16 \text{ pg m}^{-3}$ ).<sup>83</sup> However, the concentrations of N-MeFOSE in the two aforementioned coastal locations at  $0.9 \text{ pg m}^{-3}$  and  $1.2 \text{ pg m}^{-3}$ , respectively, are lower than that of the offshore location at  $2.5 \text{ pg m}^{-3}$ .<sup>83</sup>

Furthermore, the German coastline features multiple industrial and port facilities, including those in Hamburg,



Fig. 6 Atmospheric concentrations of 8 : 2 FTOH ( $\text{pg m}^{-3}$ ) in selected regions in Europe, as reported in prior studies.<sup>61,83–87</sup> Measurements in the following locations are reported: (A) German Bight, (B) Heligoland, (C) West Frisian coast, (D) Cuxhaven, (E) Schleswig-Holstein, (F) Büsum, (G) Zurich, (H) Manchester, (I) Paris, (J) Mace Head.



Bremen, and Wilhelmshaven. Jahnke *et al.* studied the atmospheric levels of fluorotelomer alcohols in Germany, revealing elevated levels of FTOH, FOSE, and FOSA in Hamburg with the maximum total concentration of FTOH reaching  $546 \text{ pg m}^{-3}$  and that of FOSE and FOSA at  $151 \text{ pg m}^{-3}$ .<sup>88</sup> Similarly, Dreyer and Ebinghaus demonstrated<sup>83</sup> high concentrations of FTOH in Hamburg, with a total concentration reaching  $180 \text{ pg m}^{-3}$ . The total concentration of all neutral PFAS studied was  $224 \text{ pg m}^{-3}$ .<sup>83</sup> Close to the German coast, near Cuxhaven, characterized by high population density and heavy industrialization, the total concentration of neutral PFAS reached  $177 \text{ pg m}^{-3}$ .<sup>84</sup> Among all the neutral PFAS compounds analyzed, 8 : 2 FTOH exhibited the highest atmospheric concentration, measured at  $75 \text{ pg m}^{-3}$  (Fig. 6 point D).<sup>84</sup> However, lower concentrations of PFAS were detected in more rural regions in Germany, such as Elbe Estuary Margin in Schleswig-Holstein ( $54.226^\circ\text{N}$ ,  $8.226^\circ\text{E}$ )<sup>84</sup> and Büsum ( $54.13^\circ\text{N}$ ,  $8.86^\circ\text{E}$ ),<sup>87</sup> with the total concentration of neutral PFAS measured  $61 \text{ pg m}^{-3}$  and  $41 \text{ pg m}^{-3}$ , respectively. As depicted in Fig. 6, the concentrations of 8 : 2 FTOH in the two regions were  $29 \text{ pg m}^{-3}$  (E) and  $25 \text{ pg m}^{-3}$  (F), respectively. Those measurements show that the rural atmosphere is influenced by transported pollution from urban and industrialized regions, reflecting background contamination. Studying this type of transported pollution further is essential to understand baseline exposure and guide control strategies.

European and North American cities are characterized by diverse industrial and consumer activities, along with growing populations.<sup>89</sup> Although several regulatory reforms have been implemented to reduce environmental PFAS levels, residual contamination and PFAS variants remain concerning.<sup>90</sup> In Zurich, Switzerland, referring to Fig. 6, significant levels of 8 : 2 FTOH were recorded at  $700 \text{ pg m}^{-3}$  (G), reflecting strong ongoing emissions.<sup>85</sup> The particle-bound concentration of PFOA ( $7.7 \text{ pg m}^{-3}$ ) was higher than that of PFOS ( $2.3 \text{ pg m}^{-3}$ ).<sup>85</sup> However, in Birmingham, United Kingdom (UK), using PAS, the level of PFOS was roughly two times greater than PFOA.<sup>91</sup> The levels could be reflective of local emission profiles and historical differences in PFAS use. In Manchester, UK, significant concentrations of particle-bound PFOA and gas-phase 8 : 2 FTOH were detected at  $341 \text{ pg m}^{-3}$  and  $237 \text{ pg m}^{-3}$  (Fig. 6 point H), respectively.<sup>61</sup> Those levels might indicate emissions from industrial activities and consumer product degradation, as well as higher exposure risk as compared to other European cities. The coexistence of elevated PFOA and 8 : 2 FTOH suggests that atmospheric degradation of volatile precursors such as 8 : 2 FTOH may contribute to PFOA formation.<sup>92</sup> In Paris, France, Rauert *et al.*<sup>86</sup> revealed high levels of FTOH in 2015, with the following trend: 8 : 2 FTOH ( $121 \text{ pg m}^{-3}$ ; Fig. 6 point I) > 6 : 2 FTOH ( $78 \text{ pg m}^{-3}$ ) > 10 : 2 FTOH ( $37 \text{ pg m}^{-3}$ ). The spatial variability observed between Zurich, Birmingham, Manchester, and Paris shows that different factors, such as local emission sources, historical usage profiles, and variations in consumer patterns, shape PFAS distribution across urban environments in Europe.

As compared to Toronto, Canada, the levels of FTOHs were lower than those of Zurich, Manchester, and Paris, and followed a slightly different trend than the one revealed in Paris: 8 : 2

FTOH ( $40.2 \text{ pg m}^{-3}$ ) > 10 : 2 FTOH ( $21.1 \text{ pg m}^{-3}$ ) > 6 : 2 FTOH ( $17.7 \text{ pg m}^{-3}$ ),<sup>46</sup> possibly attributed to differences in urban density and industrial activities. Interestingly, the particle-bound concentrations of some ionic PFAS in Albany, New York, United States of America (USA), are low with the following trend: PFOA ( $2.03 \text{ pg m}^{-3}$ ) > PFOS ( $0.64 \text{ pg m}^{-3}$ ) > PFNA ( $0.64 \text{ pg m}^{-3}$ ).<sup>93</sup> Elevated PFAS levels were detected in Cleveland, Ohio, USA, with the total concentration of 41 PFAS measured<sup>94</sup> at  $410 \text{ pg m}^{-3}$ , likely reflecting proximity to manufacturing facilities and dense traffic. While detectable PFAS levels confirm their presence in the atmosphere, these compounds remain significantly understudied in the midlatitude North American atmosphere compared to water and soil matrices. Most studies that aimed at determining the levels of PFAS in such regions tackled their detection in forms of wet deposition, rather than the gas and particulate forms, which establishes a major knowledge gap.

### 2.3. Tropical and subtropical regions

Tropical and subtropical regions are broadly characterized by warm temperatures but encompass a wide variation of precipitation patterns and seasonal conditions.<sup>95</sup> Tropical regions are localized between the Tropics of Cancer from  $23.5^\circ\text{N}$  to  $23.5^\circ\text{S}$ <sup>57</sup> (Fig. 1) and feature a hot and humid climate.<sup>95</sup> Such zones also experience heavy annual precipitation, particularly at the equatorial zones.<sup>95</sup> They host among the densest forests in the world, such as the Amazon Rainforest and the Southeast Asian Rainforests.<sup>95</sup> The concentrations of PFAS in the tropical regions generally appear to be lower than others, which could be attributed to higher rainfall and photochemical degradation.<sup>48</sup> For instance, in Hilo, Hawai'i, USA, the concentrations of many PFAS compounds were found to be below quantifiable limits.<sup>86</sup>

As for subtropical regions, they are localized between approximately  $23.5^\circ$  and  $35^\circ$  latitude in both hemispheres, bordering the tropics<sup>57</sup> (Fig. 1). Those zones are typically less humid than the tropical ones and experience warm to hot summers, along with cooler winters.<sup>57</sup> Precipitation is less consistent than the tropics, where some areas experience dryer summers than others. Some areas within this zone include the Mediterranean Basin, Northern India, parts of South America, and Southern China. Noteworthy, the subtropical latitudinal band houses many of the world's developing industrial facilities, acting as major contributors to PFAS contamination.<sup>96</sup>

However, literature on atmospheric PFAS in tropical and subtropical regions remains limited and underdeveloped, particularly in areas like Africa and the Middle East. Field measurements for atmospheric PFAS in such regions are important to better understand how desert dust influences the accumulation of these compounds. Additionally, political instability, uncontrolled industrialization, and poor environmental regulations are major drivers for the presence of atmospheric pollutants in the Middle East.<sup>97</sup> Such reasons indicate that PFAS concentrations could be significant in the regional atmosphere and quantifying the levels would serve to close some knowledge gaps.





Fig. 7 Atmospheric concentrations of 8 : 2 FTOH ( $\text{pg m}^{-3}$ ) at selected coastal East Asian locations, compiled from previous studies.<sup>96,101,102</sup> Shanghai showed the highest reported concentration among the displayed sites ( $923 \text{ pg m}^{-3}$ ).

Across Atlantic Ocean transects, extending from the equatorial, near the Gulf of Guinea, to tropical and subtropical zones in the North and South Atlantic, the changes in PFAS concentrations reflect geographic distribution and emission patterns.<sup>82</sup> Near the equatorial and south tropical Atlantic, the concentrations of 10 : 2 FTOH and 8 : 2 FTOH are relatively low, whereas that of 6 : 2 FTOH is below the detection limit.<sup>82</sup> For instance, near the Gulf of Guinea across the equatorial Atlantic, the concentrations of 10 : 2 FTOH and 8 : 2 FTOH are  $2.9 \text{ pg m}^{-3}$  and  $13 \text{ pg m}^{-3}$ , respectively.<sup>82</sup> As for the levels of FOSEs and PFOSA derivatives, they were either very low or below the detection limit.<sup>82</sup> In the Northern Atlantic, the levels of FTOHs are significantly higher, particularly 8 : 2 FTOH and 6 : 2 FTOH.<sup>82</sup>

The South China Sea industrialized coast hosts major manufacturing and production hubs in Asia.<sup>98</sup> Shenzhen, China, has experienced rapid growth in recent years, with multiple potential PFAS sources, such as textile, petrochemical, and electronic industries.<sup>99</sup> Using PAS, Liu *et al.* assessed<sup>99</sup> the levels of 11 perfluorinated compounds (PFCs) in Shenzhen's atmosphere in the fall of 2011. Their total concentrations were averaged at  $15 \text{ pg m}^{-3}$ , with the presence of all 11 PFCs at all 13 sampling sites, demonstrating pervasive PFAS pollution.<sup>99</sup> The levels of PFOA and PFOS predominated, averaging at  $5.4 \text{ pg m}^{-3}$  and  $3.1 \text{ pg m}^{-3}$ , respectively.<sup>99</sup> In the northern South China Sea, the Dongshan Marine Station is located within an atmospheric pathway influenced by northeasterly winds during winter,<sup>100</sup> facilitating the transport of PFAS from nearby industrial and urban emission sources toward the open sea. In October and from December 2019 to January 2020, Yamazaki *et al.* revealed that the sum of 12 ionic PFAS averaged at  $24 \text{ pg m}^{-3}$ , with the maximum value reaching  $33 \text{ pg m}^{-3}$ .<sup>101</sup> Both recorded in

October, the greatest detected atmospheric concentration was that of PFOA ( $9.08 \text{ pg m}^{-3}$ ), followed by that of PFOS ( $8.64 \text{ pg m}^{-3}$ ).<sup>101</sup> The levels of PFOA and PFOS appear to be higher in the Dongshan Marine Station than those in Schenzen by a factor of roughly 2–3. Although Schenzen's atmosphere is known to be heavily influenced by the semiconductor industry and consumer activities, the levels could be lower than the Dongshan Marine Station as the studies were conducted 10 years apart. It is encouraged that future work tackles data collection from various regions in China to inform policy about long-term changes in legacy PFAS concentrations. Shanghai, another major industrial and commercial zone in China, was found to suffer from high levels of atmospheric PFAS contamination.<sup>96</sup> Referring to Fig. 7, the concentrations of FTOHs were found to be significant, with 8 : 2 FTOH measured at  $923 \text{ pg m}^{-3}$ .<sup>96</sup> Referring to Fig. 7, the concentration of 8 : 2 FTOH in the Taiwan Western Strait was reported<sup>101</sup> as  $146 \text{ pg m}^{-3}$ . Near Guangdong, China, the concentrations of PFAS vary across different locations, nearshore urban-industrial, transitional offshore, and remote offshore sites.<sup>102</sup> The concentrations of 8 : 2 FTOH dominate at all three sites (Fig. 7), particularly at the two offshore sites, measured at  $40.1 \text{ pg m}^{-3}$  and  $36.2 \text{ pg m}^{-3}$ , respectively.<sup>102</sup> The levels of 6 : 2 FTOH were the lowest across all sites, but such levels are higher in the offshore locations.<sup>102</sup> The levels of 8 : 2 FTOH were high in Shanghai, likely due to measurements being collected inland near emission point sources. In contrast, concentrations in the Taiwan Strait were also elevated but lower than those in Shanghai, as the sampling sites were located near the coast. Offshore levels were lower, though not negligible, reflecting the influence of LRAT from nearby regions and emissions from shipping activities.



In Brazil, the levels of atmospheric PFAS are distributed through a tropical and subtropical gradient, extending from urban and industrialized to remote and pristine environments. São Luís do Maranhão is a major component of Brazil's Carajás mining,<sup>103</sup> petroleum refinery<sup>104</sup> and transportation<sup>105</sup> activities. As depicted in Fig. 8, Saini *et al.* revealed<sup>106</sup> that the level of atmospheric concentration of PFOA ( $24 \text{ pg m}^{-3}$ ) in the region appears to be higher than that of PFOS ( $13.2 \text{ pg m}^{-3}$ ), suggesting potential point source emissions. In Curitiba, South of Brazil, an urban environment, the concentrations of PFOS and PFOA in  $\text{PM}_{2.5}$  sampled in December 2021, ranged between  $0.013\text{--}0.29 \text{ pg m}^{-3}$  and  $0.016\text{--}0.28 \text{ pg m}^{-3}$ , respectively.<sup>107</sup> It was suggested that a possible source of PFOS could be the use of pesticide sulfluramid in the north direction to Curitiba and its transportation by wind.<sup>107</sup> Another suggested source of both PFOS and PFOA was the wastewater treatment plant affecting the atmosphere of the sampling site.<sup>107</sup> Reflecting the influence of LRAT on the accumulation of atmospheric PFAS in the Amazon Basin, the mean PFOA levels in total suspended particles throughout 24-hour sampling ranged from 0.01 to  $2.0 \text{ pg m}^{-3}$ .<sup>108</sup> Literature on the dispersion of atmospheric PFAS in Latin America remains underdeveloped and limited. A region of specific interest is the Amazon Basin that houses the largest rainforest in the world. Such environments are important as they reflect the global atmospheric circulation and cycling patterns of PFAS in tropical atmospheric systems. However, there are significant gaps in the current body of literature pertaining to the study of PFAS levels and distributions in the Amazon Basin. Future studies are encouraged to focus on expanding atmospheric PFAS data for this underrepresented region, which would fill a significant geographic and mechanistic gap in the understanding of global contamination.

### 3. Deposition patterns and mechanisms of PFAS in the atmosphere

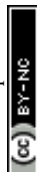
#### 3.1. Mechanism of wet deposition

Wet deposition can be defined as the removal of atmospheric pollutants by precipitation, which can include several forms, such as rain, snow, or even fog.<sup>109</sup> PFAS in fog is rarely studied in comparison to other forms. Nonetheless, some insights can be drawn from other studies focusing on PFAS in the atmosphere, as PFAS can be transported through the air and deposited *via* wet deposition. This suggests that fog, which is essentially a form of low-lying cloud, could also act as a medium for PFAS deposition. Given their surfactant-like nature, PFAS tend to adhere to the air–water interface, indicating that they could attach to water droplets in fog.<sup>110,111</sup> PFAS which can exist in both gas and particulate phase, relies mainly on wet deposition as the main removal mechanism from the atmosphere, especially for compounds like PFOA, where approximately 50–60% of deposition occurs through this mechanism.<sup>94</sup>

This removal process includes in-cloud scavenging during which PFAS or aerosols are incorporated into cloud droplets through a process called nucleation. In this process, they can act as cloud condensation nuclei (CCN) or ice nuclei (IN). Another pathway is called in-cloud impaction scavenging, which involves aerosols particles being collected with existing cloud droplets or ice crystals. These aerosols will eventually be eliminated from the atmosphere when the cloud droplet or ice particle becomes heavy enough to fall as precipitation, rain or ice.<sup>112–114</sup> Another mechanism, known as below-cloud scavenging, involves precipitating raindrops or snow particles capturing PFAS as they descend through the air beneath the



Fig. 8 Atmospheric concentrations ( $\text{pg m}^{-3}$ ) of PFOA and PFOS in São Luís do Maranhão, as reported in prior work.<sup>106</sup> The map shows that the concentration of PFOA ( $24 \text{ pg m}^{-3}$ ) is higher than that of PFOS ( $13.2 \text{ pg m}^{-3}$ ).



cloud *via* collisional interactions. Studies have shown that this type of scavenging is significantly influenced by the size distribution of falling raindrops.<sup>112,114,115</sup> In-cloud scavenging occurs when PFAS are directly incorporated into cloud droplets during condensation. These contaminated droplets eventually fall to the ground as rain or snow.

Snow deposition has been known to play a crucial role in PFAS transfer to the cryosphere and hydrosphere. Snow can effectively scavenge both particle-bound and dissolved PFAS from the atmosphere and temporarily store them until seasonal melt releases them into surface water.<sup>116,117</sup> Snow scavenging has been proven to be more efficient for long-chain PFCAs, which are often associated with sea-salt aerosols.<sup>116</sup> This phenomenon is attributed to the higher hydrophobicity of PFCAs and their tendency to associate with particulate matter and atmospheric aerosols. Interestingly, snow, due to its larger surface area, can capture both vapor-phase and particle-bound compounds, leading to more effective removal of heavier, less volatile molecules from the atmosphere.<sup>118</sup>

Wet deposition represents one of the most important processes in atmospheric cycling of PFAS, especially for ionic PFAS such as PFOA, PFNA, PFHxS, and PFOS, which are effectively non-volatile under environmental conditions and therefore rely almost entirely on snow, rain, and cloud water scavenging for atmospheric removal. Numerous studies identified wet deposition as the dominant atmospheric sink for these compounds, as Xia *et al.*, showed 60% of PFOA and 50% of the PFOA detected in the Great Lakes came from wet deposition.<sup>94</sup> Similarly, in a study conducted in South Florida, 21 legacy and emerging PFAS were detected in rainwater with PFCAs, accounting for 74% of the measured PFAS load. The consistent detection across seasons and sampling sites indicates that precipitation acts as a continuous, diffuse source of PFAS to soils, urban surfaces, and aquatic systems. The significance of this process varies to climate: in temperate regions, rainfall contributes most of the yearly downward flux, whereas in Arctic, sub-Arctic and high altitudes environments, snowfall becomes more influential because of its high scavenging efficiency, its ability to accumulate PFAS over time and its eventual release during melt events.<sup>93,110</sup> However, once deposited, volatile precursors can undergo re-volatilization, significantly increasing their residence time. On the contrary, ionic PFAS, exhibit extremely low vapor pressures, hindering their re-volatilization from dry surfaces. They typically re-enter the atmosphere indirectly, *via* sea spray aerosols or wildfire smoke. Re-volatilization is influenced by several factors and environmental conditions such as temperature, humidity and the chemical properties of the compounds themselves. Higher temperatures can increase the volatility of PFAS, especially short-chain compounds, enabling them to easily transition from particulate to gas phase.<sup>94</sup> Moreover, relative humidity also plays a pivotal role. Higher relative humidity leads to the adsorption of water molecules, inducing competition for adsorption sites on soil minerals, and weakening PFAS-soil interaction.<sup>119</sup> Moreover, PFAS sorption and desorption can vary depending on the surface properties, such as the soil type, organic content, and surface roughness. Surfaces with high

organic carbon bind PFAS more strongly, preventing the re-volatilization of precursors, while sandy soil will bind PFAS weakly.<sup>120</sup> This re-volatilization process can significantly affect long-term environmental exposure to PFAS. As PFAS re-enter the atmosphere, they can be transported over long distances and deposited again through wet or dry deposition, perpetuating their presence in the environment.<sup>121</sup> This cyclical process contributes to the persistence and widespread distribution of PFAS making them challenging to manage and mitigate. Sea Spray Aerosols (SSA) play a crucial role in the atmospheric transport and deposition of long-chain PFCAs. These aerosols are generated from the ocean surface and serve as carriers for PFCAs, especially those with longer chains and surfactant properties. During the formation of sea sprays, long-chain PFCAs tend to partition preferentially into the surface microlayer and are subsequently ejected into the atmosphere through bubble bursting mechanisms.<sup>121</sup> Once airborne, these substances become adsorbed onto SSA particles, serving as an efficient condensation nuclei for snowfall. A study conducted by Johansson *et al.* (2019) demonstrated that enrichment factor (EF), defined as the ratio of the concentration in the surface microlayer (SML) to the concentration in the bulk seawater, was significantly higher for long chain PFCAs in SSA compared to short-chain compounds. The SML EF ranged from 13 to 47 for long chain PFCAs, while short chain PFCAs had much lower values with factors of 1.2–2.9 for C<sub>9</sub> compounds and 1.1–1.2 for C<sub>6</sub> PFCAs.<sup>121</sup> Moreover, a study conducted in Antarctica detected only PFCAs at quantifiable levels, while shorter chain PFAS were below detection limits.<sup>122</sup> These results indicate that snowfall selectively scavenges long-chain PFAS because they partition more strongly to SSA. This pattern was also highlighted by Casal *et al.* (2017), who also reported the highest concentrations for PFCA homologues.<sup>116</sup> Collectively, these studies highlight the role of chain length in enrichment mechanisms, where the longer chain compounds efficiently partition into SML and are transferred to SSA. Once transferred, the compounds can travel long distances to remote regions, such as Antarctica.

Furthermore, FTOHs and FTAs are not necessarily permanently removed from the atmosphere. Instead, they can re-volatilize after deposition. For instance, flux measurements of FTOHs and FTAs have shown positive air-snow exchange, especially in warmer conditions, indicating re-emission from snow to air during the summer, reaching 118 pg m<sup>-2</sup> d<sup>-1</sup>.<sup>48</sup> A 2023 study on Svalbard's surface suggested that both FTOHs and FTAs can be released from snow after deposition, driven by warming temperatures and melting snow.<sup>117</sup> These findings show that snowpacks may act as temporary PFAS reservoirs, particularly during the summer, contributing to secondary PFAS pollution.

In summary, wet depositions play a critical role in the atmospheric removal and redistribution of PFAS, particularly long-chain compounds. Snow has been proven to be highly efficient for PFAS scavenging due to its large surface area and capacity to trap both gas-phase and particle-phase compounds. Sea spray aerosols further contribute to atmospheric loading of PFAS, serving as carriers for surface-enriched long-chain compounds. However, the notion that snow serves as



a permanent sink is increasingly challenged by studies revealing re-volatilization of PFAS during warmer periods, highlighting the transient nature of snowpacks as PFAS reservoirs.

Nevertheless, several gaps still remain in PFAS wet deposition literature. For instance, the role of fog as a deposition pathway remains underexplored, especially in urban and coastal areas. Moreover, despite their rising prevalence and distinct mobile behavior, short-chain and emerging PFAS are less studied than legacy long-chain ones.

### 3.2. PFAS in rain, snow, and ice

Wet deposition removes PFAS unevenly, depending on climate, precipitation chemistry, and compound properties. In temperate and mid-latitude regions, rainfall is generally the dominant contributor due to its high frequency and cumulative volume. At larger regional scale, long-term Great Lakes monitoring reported median PFOS and PFOA concentrations of  $0.93 \text{ ng L}^{-1}$  and  $0.49 \text{ ng L}^{-1}$ , respectively, in bulk precipitation. In contrast, snow becomes the primary scavenging mechanism in polar environments, exhibiting higher PFAS enrichment per unit of precipitation. Kim and Kannan<sup>93</sup> reported PFAA concentrations of  $0.91\text{--}13.2 \text{ ng L}^{-1}$  in rain and  $0.91\text{--}23.9 \text{ ng L}^{-1}$  in snow, indicating comparable or slightly higher levels in snow.<sup>93</sup> Arctic surface snow typically contains  $0.007\text{--}0.4 \text{ ng per L}$  PFOA.<sup>110</sup> Furthermore, snowpacks accumulate PFAS seasonally and release them rapidly during melt, generating concentrated pulses to downstream ecosystems. At maritime Antarctic sites, PFAS in snow are consistently higher than in seawater, demonstrating that snow is an efficient scavenging and temporary storage mechanism, particularly for long-chain PFAAs with low vapor pressure<sup>116</sup>

Table 2 shows the concentration of PFAS in rain, ice and snow as well as deposition flux among various locations of sampling. Precipitation-based sampling shows PFAS are ubiquitous in atmospheric deposition, even in remote regions. For instance, rainwater studies in Japan, show measurable concentrations of PFAS at several intervals during single rainfall events, with the total flux ranging from  $40.8$  to  $186 \text{ ng per m}^2$  per day (Table 2). The major PFAS compounds found in rainfall were PFBA, PFNA and PFOA, indicating continuous atmospheric scavenging of PFAS away from sources.<sup>123</sup> Moreover, a study conducted in Wilmington, USA detected a total PFAS concentration reaching  $110 \text{ ng L}^{-1}$  in rainfall along with a deposition flux of  $0.3\text{--}29 \text{ ng per m}^2$  per day.<sup>124</sup> Moreover, another study conducted in Wisconsin as part of the National Atmospheric Deposition Program reported the detection of  $1.3$  to  $47.4 \text{ ng per m}^2$  per day PFAS flux.<sup>125</sup> Complementary to these findings, Kim and Kannan (2007)<sup>93</sup> reported notable PFAS concentrations in rainfall and lakes from various locations across the United States. PFOA concentrations in urban lakes ranged between  $4.38$  and  $15.8 \text{ ng L}^{-1}$ , while lower levels were detected in rural areas, ranging between  $1.24$  and  $3.87 \text{ ng L}^{-1}$ . European data reveal a similarly wide range of concentrations: in Germany, the major PFAS compounds detected in rain were PFOA and PFBA with a total PFAS concentration of  $1.6$  to

$48.6 \text{ ng L}^{-1}$  and a deposition flux ranging from  $2$  to  $91 \text{ ng per m}^2$  per day.<sup>126</sup> Similarly, Han *et al.* (2019) documented substantial variability in PFAS concentrations in precipitation samples from cities across China, linking elevated levels directly to fluorochemical manufacturing activities. Measurable PFAS concentrations were also detected at rural background sites.<sup>74</sup> In the study, PFAS variations depended on their local source emissions as well as regional atmospheric transport. Additionally, the total annual wet deposition fluxes reported in Chinese urban areas are significant, with one study reporting a total of  $14.3 \text{ ng per m}^2$  per day, dominated by PFBA ( $4.93 \text{ ng per m}^2$  per day) and PFOA ( $3.29 \text{ ng per m}^2$  per day), followed by PFOS and other PFCAs<sup>127</sup>

When compared, these studies illustrate both strong points of agreement and notable contradictions across regions. A consistent trend is the dominance of short-chain PFCAs, especially PFBA, in rainfall, supporting the growing scientific consensus that these more mobile compounds are increasingly present in the atmospheric PFAS pool as industries phase-out long chain PFAS. However, the large variability in reported concentrations and fluxes ranging from a few  $\text{ng per m}^2$  per day in rural areas to almost  $100 \text{ ng per m}^2$  per day near urban or industrial centres highlights how wet deposition is strongly shaped by local atmospheric chemistry, precursors, meteorological conditions and proximity to sources such as local industries and urban activities.<sup>93</sup> Methodological differences in both sampling and analysis may also contribute to this variability. Sampling approaches vary in whether they are event-based or cumulative, as well as in the type of precipitation collected. Analytical differences include variations in detection limits and the range of analytes targeted in each study.

Snow cores from the Arctic and Antarctic confirm deposition of diverse PFAS, including long- and short-chain PFCAs, PFSAs, and replacements like HFPO-DA (GenX), highlighting LRAT.<sup>117</sup> Snow cores are particularly valuable as environmental archives, providing historical records for global PFAS distribution and atmospheric deposition trends over decades. For instance, analysis of ice cores from the Devon Ice Cap in the Canadian Arctic revealed increasing PFAS concentrations starting in the mid-1980s, corresponding closely with the global industrial-scale production and use of PFAS compounds.<sup>129</sup> Deposition in the Arctic showed positive correlations with solar flux, which can suggest a strong photochemical formation pathway from volatile precursors like FTOHs and sulphonamide compounds.<sup>110,117</sup> Notably, deposition fluxes during 24-hour daylight periods were  $7.9$  to  $71$  times higher than those collected during dark periods.<sup>117</sup> Collectively, these snow-core-derived data offer unique insights into historical emissions, global dispersion patterns, and the effectiveness of regulatory actions over time. Some of these regulations include usage restrictions such as the Toxic Substance Control Act (TSCA) imposed by the EPA, requiring companies to notify the EPA before manufacturing or importing certain types of PFAS.<sup>131</sup> Moreover, the EPA is proposing bans or restrictions on the most hazardous PFAS as a part of the PFAS Strategic Roadmap. The 2023 Proposal includes the ban on most uses of PFOA, PFOS, PFNA, and GenX.<sup>132</sup> Additionally, in Europe, several PFAS, including



Table 2 The concentration of PFAS in rain, ice and snow as well as deposition flux among various locations of sampling

Author	Location of sampling	Period of sampling	Types of PFAS compound measured	Type of precipitation studied	Concentration in rain of $\Sigma$ PFAS/ice/snow (ng L <sup>-1</sup> )	Deposition flux (ng per m <sup>2</sup> per day)
Pfotenhauer <i>et al.</i> , 2022 (ref. 125)	Wisconsin, USA (upper Great Lakes Location)	5 Months	34 per- and polyfluoroalkyls (PFAS), mainly PFCAs	Rain	0.7–6.1 (median 1.5)	1.3–47.4 (median 5.7)
Wang <i>et al.</i> , 2022 (ref. 128)	Chongqing, China (metropolitan, subtropical)	July 2020–April 2021 (4 seasons)	PFBA, PFPeA, PFHxA, PFHpA, PFOA, PFNA, PFDA, PFUDA, PFDoA, PFTyDA, PFTeDA, PFHxDA, PFODA, PFBS, PFHxS, PFOS, PFDS (17)	Rain	3.31–196.14	13.9
Hartz <i>et al.</i> , 2023 (ref. 110)	Lomonosovfonna Ice Cap, Svalbard, Norway (High Arctic)	A decade, 2007–2018	TFA, PFOS, C2–C11 PFCAs (45 targeted, 26 detected)	Ice core	9.51–16,500	0.0068–22.45
Taniyasu <i>et al.</i> , 2013 (ref. 123)	Japan (Tsukuba, Mt. Tateyama, Pacific Ocean)	During seven rainfall events: 1 July 2006	PFBS, PFCAs, FTOHs	Rain; surface snow; snow core	Rain: NR, surface snow: 3.04–40.5 Snow core: 0.884–4.51	40.8–186
S. Wang <i>et al.</i> , 2022 (ref. 127)	Xiamen, China (Subtropical)	12 December 2006				
Maclinnis <i>et al.</i> , 2017 (ref. 129)	Devon Ice Cap, Canada	16 April 2007				
Young <i>et al.</i> , 2007 (ref. 130)	Arctic Ice Caps (North)	10 June 2007				
Dreyer <i>et al.</i> , 2010 (ref. 126)	Northern Germany	14 June 2007				
Shimizu <i>et al.</i> , 2021 (ref. 124)	Wilmington, USA	19 October 2007				
Casal <i>et al.</i> , 2017 (ref. 116)	Livingston Island, Maritime Antarctica	12 January 2008				
		1 Year	PFOS, PFOA, PFBA, 6 : 2 Cl-PFESA (4)	Rain	0.20–180.65 (average 10.71)	14.24
		14 Years (1993–2007)	PFBA, PFECBS, PFAAs (PFCAs, PFSAs), FOSA	Snow Pit	NR	<0.003–0.8
		1996–2005	PFOA, PFNA, PFDA, PFUnDA, PFOS	Snow core	Low to mid pg L <sup>-1</sup>	0.42
		7 months (2007–2008)	PFOA, PFBA (34)	Rain	1.6–48.6	2.0–91
		December 2018–December 2019 (1 year)	PFOS, PFOA, PFECAs, HFPO-DA, PFMOBA, PMPA	Rain	LOQ-110	0.3–29
		December 2014–February 2015	PFCAs (PFOA, PFNA), PFSAs (PFOS)	Snow	0.76–3.6	NR



PFOA, PFOS, and PFHxS are restricted or banned under the Stockholm Convention.<sup>133</sup> While these measures would contribute to the reduction of PFAS use in developed countries, they reflect a growing global divide. While both the United States and Europe have implemented strict restrictions on PFAS production and use, many developing countries that often lack these regulatory infrastructures or economic leverage remain vulnerable to both unregulated PFAS usage and transboundary atmospheric transport of PFAS emitted elsewhere.

In European alpine regions, snow samples taken from the Ortles glacier revealed PFBA in dominance in surface layers, which is consistent with its widespread current use and high

mobility. Deeper layers showed increased concentrations of PFOA and PFNA, reflecting post-depositional migration driven by meltwater percolation.<sup>116</sup> This process selectively removes short-chain PFAS, while retaining longer chains, modifying the chemical profile with depth.<sup>134</sup> Remote snow records from the Devon Ice Cap in Canada showed that annual PFCA fluxes increased after 1985, peaking in the 2000s, and declined slightly post 2012, which is due to the US EPA's PFOA Stewardship Program and Canadian Environmental Agreements<sup>134</sup> (Fig. 9). However, deposition of short-chain PFAS such as PFBA has continued or even increased, highlighting the ongoing global shift toward short-chain replacements.<sup>134,135</sup>



Fig. 9 The annual deposition fluxes of PFOA (a) and PFNA (b) in ng per m<sup>2</sup> per year on the Devon Ice Cap. The solid black line represents the 5-year moving average. Reproduced from Pickard *et al.*,<sup>134</sup> sourced from *Atmospheric Chemistry and Physics*, licensed under CC BY 4.0, available online at DOI: <https://doi.org/10.5194/acp-18-5045-2018>.



The Tibetan Plateau, often referred to as Earth's "Third Pole", presents another instructive case. Despite its remoteness, regions like Tianshan and Laohugou have recorded elevated PFAS concentrations in snow of 2.35 ng L<sup>-1</sup> and 2.3 ng L<sup>-1</sup>, respectively, attributed to long-range transport from South and East Asian industrial centres.<sup>135</sup> Similarly, a study conducted by Casal *et al.* (2017) reported concentrations ranging from 0.76 to 3.6 ng L<sup>-1</sup> in freshly deposited snow and a concentration of 0.082 to 0.43 ng L<sup>-1</sup> in surface snow on Livingston island<sup>116</sup> (Table 2). Even near the summit of Mount Everest (~8850 m), measurable levels of PFAS in snow were detected, with PFOS and PFOA reaching concentrations of 26.4 ng L<sup>-1</sup> and 2.14 ng L<sup>-1</sup>, respectively. These findings highlight the remarkable vertical extent of PFAS atmospheric dispersion.<sup>136</sup> Similarly, in the Arctic region, PFOS and PFOA were the most prominent PFAS with a concentration range of 0.003–0.086 ng L<sup>-1</sup> and 0.014–0.147 ng L<sup>-1</sup>, respectively. In European Alps, the major PFAS found were PFOA with a concentration ranging from 0.2 to 0.6 ng L<sup>-1</sup> and PFBA with concentrations from 0.3 to 1.8 ng L<sup>-1</sup>.<sup>137</sup> Additionally, Young *et al.* (2007) quantified PFAS in snowpacks in the Arctic region, finding concentrations ranging from low to mid pg L<sup>-1</sup> with a deposition flux of 0.42 ng per m<sup>2</sup> per day (ref. 130) (Table 2). PFAS in remote regions highlight their persistence and mobility, driven by atmospheric transport and gas–particle partitioning.

To conclude, the global scale presence of PFAS in atmospheric deposition from urban rainfall in the U.S and Germany to snowpacks in the Arctic, Antarctic, and high-altitude regions like the Himalayas underscores their persistence, mobility, and long-range transport potential. Precipitation acts as both a transport medium and temporary reservoir, with snow preserving long-term deposition trends linked to industrial activity and regulation. Despite regulatory actions in many industrialized nations, the continued detection of PFAS, in remote and high-altitude environments indicates ongoing global emissions and gaps in enforcement or substitution strategies.

While annual cumulative deposition fluxes are often reported, high-resolution, event-based deposition data from diverse regions are scarce, which limits temporal trend analyses and source attribution. Standardization of sampling and analysis techniques is also necessary to provide a more nuanced approach in PFAS regulation. Additionally, no published study has quantified the percentage of total atmospheric PFAS wet deposition to each precipitation type (rain, snow, fog) in a globally representative way. While numerous datasets report concentrations or fluxes in rain *versus* snow, the absence of systematic, region-wide comparative data means that we cannot yet assign a definitive share to any single precipitation form.

### 3.3. Atmospheric implications and transport pathways

The efficiency of PFAS scavenging through precipitation has significant implications on atmospheric fate and transport. Typically, scavenging efficiency for particle-bound PFAS often exceeds 70%, especially during rainfall seasons.<sup>67</sup> However, the effectiveness varies by compound and environmental<sup>127</sup>

conditions. For instance, short-chain volatile PFAS may evade removal during light rain and remain airborne longer, enhancing their potential for long-range transport. This is primarily due to their higher vapor pressure and lower water solubility compared to long-chain PFAS, which makes them less likely to be scavenged by raindrops. As a result, these compounds can persist in the atmosphere and travel considerable distances before eventually undergoing oxidation or deposition in remote regions.<sup>25,79</sup> The source–receptor dynamics of PFAS are evident in studies where deposition fluxes decrease exponentially with distance from point sources such as fluorochemical plants or waste treatment facilities.<sup>79</sup> In some cases, air concentrations of 8 : 2 FTOH and PFOA declined by 98–90% within just 5 km of an industrial source, whereas short-chain PFAS remained detectable even 40 km away.<sup>94</sup>

One key insight from global deposition studies is that depositions represent a sink for atmospheric PFAS but a source of PFAS for surface systems such as soils or water. While precipitations remove PFAS from the atmosphere, these compounds are then introduced to land, snow, and water where they accumulate.<sup>94,138</sup> These dual roles complicate risk management efforts, as removing PFAS from the atmosphere does not prevent accumulation in surface systems.

Once PFAS are deposited from the atmosphere, they often reach aquatic environments *via* direct precipitation, snowmelt, or runoff. This process is well documented in both urban and remote settings. In the Great Lakes region, atmospheric deposition accounts for over 90% of PFAS input to Lake Superior, despite its size and distance from point sources.<sup>94</sup> Another study conducted by Filipovic *et al.* (2015) in a pristine region in Sweden found a positive mass balance of PFAS in the riverine. Atmospheric deposition contributes to aquatic PFAS directly and indirectly through soil accumulation and subsequent transport to surface waters. Since these compounds do not readily degrade, they tend to accumulate in soil through atmospheric deposition before being transferred to the surface waters, confirming that major pathway of PFAS entry into the Baltic Sea is *via* deposition.<sup>139</sup> These results could also be confirmed by a study in Canada where snowpacks were proven to be a significant temporary PFAS reservoir during the winter. These molecules accumulate in snow layers due to atmospheric deposition, effectively concentrating contaminants until spring melt.<sup>140</sup> Other lakes, such as Michigan and Huron, exhibit net accumulation of PFAS, reflecting sustained inputs for atmospheric deposition, surface runoff, and tributary inflows. This net accumulation in large lakes often results from limited outflow, relatively slow flushing rates, and high watershed-to-lake surface area ratios, which collectively enhance retention.<sup>94</sup> Codling *et al.* (2018) further confirm these patterns, reporting that Lake Michigan sediment cores clearly document the persistent PFAS accumulation over recent decades.<sup>141</sup> In contrast, Lakes Erie and Ontario exhibit net exporters, effectively removing PFAS through hydrological outflow rather than accumulation in sediments.<sup>94</sup>

The efficiency of PFAS scavenging by precipitation plays a pivotal role in determining their atmospheric residence time, transport range, and eventual deposition patterns. While long-



chain, particle-bound PFAS are effectively removed during rainfall events, short-chain, volatile compounds often escape such removal and remain airborne, facilitating LRAT. Importantly, atmospheric deposition functions as both a removal pathway from the air and a significant source to terrestrial and aquatic ecosystems. Numerous studies from the Great Lakes, Sweden, and Canada have demonstrated that deposited PFAS accumulate in snowpacks, soils, and surface waters often serving as long-term reservoirs. These deposits can be remobilized through snowmelt, runoff, or slow flushing, especially in large water bodies with high retention capacity like Lake Superior and Lake Michigan. In contrast, lakes with higher outflows, such as Erie and Ontario, may exhibit net PFAS export. Ultimately, while atmospheric deposition reduces airborne PFAS burdens, it contributes substantially to their environmental persistence and complexity in downstream ecosystems. This dual role underscores the importance of integrating atmospheric and hydrological models in PFAS risk assessments and environmental management strategies.

## 4. PFAS transformations and phase partitioning in the atmosphere

### 4.1. Atmospheric transformation and reactivity of PFAS precursors

PFAS emitted from point-source regions could travel to remote environments *via* LRAT.<sup>48</sup> This phenomenon has been frequently observed for persistent pollutants, where they travel from warmer regions and point sources to polar regions, where they tend to accumulate. To clarify, the levels of different FTOH chain lengths have been demonstrated to be a marker for LRAT, with high ratios of 8:2 to 10:2 to 6:2 FTOH near polar regions.<sup>48</sup> Xie *et al.* found an elevated ratio of 8:2 to 10:2 to 6:2 FTOH near the Arctic, demonstrating the significant role of LRAT.<sup>49</sup> Over the northeastern Atlantic Ocean, the levels of FTOHs were revealed<sup>142</sup> to be inconsistent across measured samples, with strong influence from land-based contributions as the highest recorded level was 156 pg m<sup>-3</sup>. Such fluctuations indicate that local emission sources, such as industrialization, highly contribute to the levels of FTOHs in the studied marine environment and hinder uniform distribution. In the Tibetan Plateau, a remote region, the concentration of neutral PFAS tends to be high, particularly 8:2 FTOH, due to LRAT from industrial regions.<sup>60</sup> In fact, the relative ratios of 8:2, 10:2, and 6:2 FTOHs further demonstrate the aging of air masses in remote regions, in contrast to fresher emissions near cities.<sup>60</sup>

Although the main source of PFAS in Arctic regions is LRAT, marine aerosols are considered to be another source that could be dependent on several external factors. Sha *et al.* revealed seasonal variations to the contribution of sea spray to PFAS as it appears to be higher than that of precursor degradation in the winter.<sup>138</sup> In winter, wind-driven transfers from the ocean to the atmosphere are more consistent and the concentrations of OH radicals seem to be limited, inhibiting atmospheric oxidation of volatile PFAS.<sup>138</sup> However, in summer, photochemical transformations become more important contributors due to the

increase in the activity of atmospheric oxidation pathways.<sup>138</sup> This is consistent with the finding presented by a study that sampled ice cores from the Devon Ice Cap, Devon Island, Nunavut, where there seems to be minimal contribution from marine aerosols in the sampling month of May.<sup>134</sup>

Moreover, a study was conducted to examine the historical trends of atmospheric oxidation of polyfluorinated amides (PFAMs) and their potential as contributors to PFCAs and PFOA.<sup>143</sup> It was revealed that *N*-ethylperfluorobutyramide (EtFBA) could be oxidized rapidly by both chlorine and hydroxyl radicals, with a lifetime of roughly 4.4 days with the latter.<sup>143</sup> The degradation products included perfluorobutyramide (C<sub>3</sub>F<sub>7</sub>C(O)NH<sub>2</sub>), TFA, PFPrA, and PFBA.<sup>143</sup> Remarkably, PFCA formation was also revealed from the oxidation of intermediate fluorinated radicals, which leads to the release of COF<sub>2</sub> through sequential transformations and the eventual production of stable PFCA end-products.<sup>143</sup> It was suggested that Arctic branched PFOAs are the result of PFAM oxidation, instead of environmental transport.<sup>143</sup>

Although methyl perfluorobutane sulfonamidoethanol (MeFBSE) is highly reactive and degrades quickly in the atmosphere, elevated concentrations were identified in Antarctica.<sup>50</sup> This unexpected finding could suggest the presence of distant point sources, LRAT, or degradation of certain precursor compounds.<sup>50</sup> Interestingly, MeFBSE and methyl perfluorobutane sulfonamide (MeFBSA) are precursors for the formation of short-chain perfluoroalkyl acids, which are resistant to further transformations.<sup>50</sup> Their highly persistent properties and their water solubility result in their detection in Antarctic surface waters.<sup>50</sup> The pathways leading to the formation of short chain in the atmosphere remain underdeveloped in the literature. Future research tackling this knowledge gap is important to understand the persistence of short chain PFAS, considering the increase in usage and production in industries due to shifts in policy regulations worldwide.

The transformations and atmospheric behavior of PFAS could be understood through their occurrence in Arctic snow.<sup>130</sup> It seems that PFAS are the greatest in the spring and summer seasons, which could be attributed to increased photochemical reactions that enhance the atmospheric oxidation of volatile precursors into PFAS.<sup>130</sup> Interestingly, although long-chain PFDA and PFUnDA are commercially limited, their occurrence in the High Arctic could suggest their production *via* atmospheric oxidative reactions.<sup>130</sup> Those oxidation pathways are supported by association study. For instance, the oxidation of 8:2 FTOH could be attributed to the strong positive correlation between PFOA and perfluorononanoic acid (PFNA).<sup>130</sup> For PFDA and PFUnDA, which showed near-identical correlation, their shared precursor appears to be 10:2 FTOH.<sup>130</sup> It seems that atmospheric oxidation is the dominant mechanism driving the transport and deposition of PFAS in the Arctic. In a study conducted in North Greenland, higher levels of neutral PFAS were revealed in the summer as compared to late winter seasons, in which it was suggested that re-emission processes from snowpack are a secondary source of PFAS after LRAT.<sup>53</sup>

The major atmospheric sink of FTOHs in the atmosphere is OH radicals, which was shown to react primarily with the alpha-



CH<sub>2</sub>-group adjacent to the hydroxyl of FTOH.<sup>144</sup> Although Cl atoms have been shown to be roughly 15 folds more reactive with FTOHs than OH radicals, their occurrence in the troposphere seems to be low.<sup>144</sup> This notion explains why transformations with Cl atoms are considered minor atmospheric sinks for FTOHs. FTOH appears to perform LRAT, reaching remote regions, due to its estimated atmospheric lifetime of 20 days.<sup>144</sup>

Much of the literature has revealed that the reaction between Cl atoms and CF<sub>3</sub>(CF<sub>2</sub>)<sub>3</sub>CH<sub>2</sub>CH<sub>2</sub>OH (4 : 2 FTOH) selectively targets the alpha-CH<sub>2</sub>-group adjacent to the hydroxyl to produce C<sub>4</sub>F<sub>9</sub>CH·OHCH<sub>3</sub>.<sup>145,146</sup> This radical subsequently reacts with O<sub>2</sub> to form the primary product, CF<sub>3</sub>(CF<sub>2</sub>)<sub>3</sub>CH<sub>2</sub>CHO.<sup>145</sup> Secondary oxidation products, CF<sub>3</sub>(CF<sub>2</sub>)<sub>3</sub>CHO and CF<sub>3</sub>(CF<sub>2</sub>)<sub>3</sub>CH<sub>2</sub>COOH (2*H*, 2*H*-perfluorohexanoic acid or 4 : 2-FTCA) can also be formed through peroxy radical pathways. The products reveal one of the oxidative mechanisms of FTOH into more persistent PFAS. When irradiating a mixture of a fluorinated alcohol with chlorine in the presence of NO<sub>x</sub>, results from IR spectroscopy revealed the formation of primary products, formic acid and fluorinated aldehydes (C<sub>4</sub>F<sub>9</sub>CH<sub>2</sub>CHO, and C<sub>4</sub>F<sub>9</sub>CHO), as well as residues of fluorinated organic nitrates and/or nitrites.<sup>147</sup> As such, in the presence of NO<sub>x</sub>, C<sub>4</sub>F<sub>9</sub>CH<sub>2</sub>CHO was revealed to be a significant product of 4 : 2 FTOH oxidation,<sup>147</sup> but not the only one, unlike that in the absence of NO<sub>x</sub>.<sup>145</sup>

In agreement with the aforementioned studies, through IR spectroscopy, the Cl-initiated oxidation of C<sub>8</sub>F<sub>17</sub>CH<sub>2</sub>CH<sub>2</sub>OH (8 : 2 FTOH) results in the formation of C<sub>8</sub>F<sub>17</sub>CH<sub>2</sub>CHO.<sup>148</sup> The mechanism involves a hydrogen abstraction from the -CH<sub>2</sub>OH from the reaction between Cl and C<sub>8</sub>F<sub>17</sub>CH<sub>2</sub>CH<sub>2</sub>OH, resulting in C<sub>8</sub>F<sub>17</sub>CH<sub>2</sub>CHOH radical.<sup>148</sup> This step is followed by the reaction between the radical and oxygen, resulting in the formation of the fluorinated aldehyde, C<sub>8</sub>F<sub>17</sub>CH<sub>2</sub>CHO.<sup>148</sup> The formation of a perfluorinated aldehyde product from the reaction between perfluorinated alcohols with Cl atoms was also presented in the study by Solignac *et al.* as a primary product, but CO and CF<sub>2</sub>O appear to be produced later in the reaction as secondary products.<sup>149</sup>

It was shown that the chain lengths of FTOHs might have minimal influence on the degree of reactivity with OH radicals and Cl, particularly the reaction rate constant.<sup>144</sup> This finding can be explained by considering that the oxidant reacts with the CH<sub>2</sub> group rather than the carbon-fluorine chain. However, perfluorinated acid products of Cl atom-initiated oxidation of FTOH in the air with low levels of NO<sub>x</sub> vary with the chain length of the reactant FTOH.<sup>150</sup> For instance, 8 : 2 FTOH appears to be a precursor for the production of PFNA, PFOA, pFHpA, PFHxA, PFPeA, PFBA, PFPrA, and TFA, while 6 : 2 FTOH is a precursor for all the acids, except for PFNA and PFOA.<sup>150</sup>

The formation of C<sub>7</sub>F<sub>15</sub>COOH (PFOA) from longer chain FTOH appears to be environmentally significant due to its high persistence and stability. Simulation has shown that the rate of PFOA formation from FTOH degradation is 0.88 Gg per year (ref. 151) which is roughly estimated to be 15% of the total PFOA global source flux.<sup>151</sup> PFOA is one of the PFCAs that could be formed from the oxidative pathway of 8 : 2 FTOH, which primarily reacts with OH radicals.<sup>92</sup> This initial reaction results

in the formation of perfluoroaldehyde, which undergoes further oxidation to form C<sub>8</sub>F<sub>17</sub>C(O)O<sub>2</sub> and C<sub>8</sub>F<sub>17</sub>O<sub>2</sub> radicals.<sup>92</sup> Subsequent reactions with HO<sub>2</sub> and CH<sub>3</sub>O<sub>2</sub> result in the formation of PFCAs, including PFOA and PFNA.<sup>92</sup> Significantly, levels of PFOA appear to be higher in remote regions than source locations since the concentration of NO<sub>x</sub> is higher in the latter.<sup>92</sup> The dependence of the PFOA levels on NO<sub>x</sub> concentration is attributed to the reaction between C<sub>8</sub>F<sub>17</sub>O<sub>2</sub> and NO that competes with the reaction producing PFOA.<sup>92</sup> This pattern has also been discussed<sup>152</sup> by Yarwood *et al.*, claiming that the PFOA yield is dependent on the rates of C<sub>8</sub>F<sub>17</sub>O<sub>2</sub> with NO and RO<sub>2</sub>. For instance, the comprehensive air-quality model with extensions showed the lowest PFOA yields, in July, over the Ohio Valley, a NO<sub>x</sub> abundant region.<sup>152</sup>

Quantum chemical calculations by Sun *et al.* were performed<sup>153</sup> to investigate the OH-induced oxidative degradation process of *n* : 2 FTOH. Abstraction of H atoms from the alpha-CH<sub>2</sub>-group adjacent to the hydroxyl was revealed to be thermodynamically favored process.<sup>153</sup> The thermodynamic barrier was also found to slightly increase with carbon chain length.<sup>153</sup> The increased stability of the C-F bond was revealed to be attributed to the high Gibbs free energy barrier of F-abstraction by OH.<sup>153</sup> In fact, the strength of the C-F bond is a well-established concept in the literature.<sup>154,155</sup> This resistance to defluorination attributes to the highly stable nature of the oxidation products. Consistently, Altarawneh & Dlugogorski utilizing a model compound (CF<sub>3</sub>CF<sub>2</sub>CH<sub>2</sub>CH<sub>2</sub>OH) to represent atmospheric oxidation of FTOH,<sup>156</sup> identified the same initial Hydrogen abstraction step, forming the CF<sub>3</sub>CF<sub>2</sub>CHCH<sub>2</sub>OH radical.<sup>156</sup> Following the abstraction, the radical reacts with oxygen to form CF<sub>3</sub>CF<sub>2</sub>CH(OH)CH<sub>2</sub>OO, which after unimolecular elimination of HO<sub>2</sub> produces the aldehyde intermediate CF<sub>3</sub>CF<sub>2</sub>CH<sub>2</sub>CHO.<sup>156</sup> Further oxidation of the aldehyde produces CF<sub>3</sub>CF<sub>2</sub>CH<sub>2</sub>C(O)O<sub>2</sub>, which reacts with HO<sub>2</sub> to produce PFCA.<sup>156</sup> Plumlee *et al.* suggested a reaction pathway for the formation of FOSAs and PFOA from the degradation of N-EtFOSE through OH oxidation and *N*-dealkylation, a form of indirect photolysis.<sup>157</sup> Blanco *et al.* also showed that the reactions of fluoroacetates with Cl in the atmosphere contribute to the formation of fluoroacetic acid through a structural rearrangement of the ester moiety with a five membered ring intermediate.<sup>158</sup> Those studies show the role of photooxidation processes in the formation of more persistent forms of PFAS.

#### 4.2. Sorption behavior and phase distribution of PFAS in the atmosphere

Much of the current literature agrees that the partitioning of atmospheric PFAS is governed primarily by functionalization, volatility, and chain length. Although volatile PFAS are generally found predominantly in the gas phase, their degree of particle association varies according to their physicochemical properties.<sup>87</sup> For example, FTOHs show the weakest particle affinity (<8% particle-bound fraction), FOSEs exhibit substantially higher particle association (average 15.5%, up to 30.6%), and FTAs and PFOSA derivatives display more intermediate partitioning behavior.<sup>87</sup> This implies that FTOHs might exhibit



longer presence in the atmosphere as they partition better in the gas-phase, whereas FOSEs could experience less LRAT due to settling or deposition. Similarly, in field observations, the percentage of partitioning to particle phase followed this trend: MeFOSE > 8 : 2 FTOH > EtFOSE > 10 : 2 FTOH > 6 : 2 FTOH.<sup>46</sup> This trend was associated with volatility, where less volatile compounds could associate better to particles.<sup>46</sup> However, an exception to this trend appears to be 8 : 2 and 10 : 2 FTOH as 8 : 2 showed greater particle association even though it is more volatile, which could be attributed to experimental variability.<sup>46</sup>

The main contributors to PFCAs in the atmosphere are the oxidation of fluorinated precursors and point source emissions from industrialization and consumerism.<sup>159</sup> The low volatility and increased functionalization of PFAAs result in their high affinity to the particulate phase rather than the gas phase.<sup>159</sup> PFOA and PFBA had the highest levels, suggesting that these compounds could be more effectively partitioned in the particulate phase.<sup>159</sup>

The illustrated spectrum (Fig. 10) visually summarizes the atmospheric partitioning behavior of volatile and ionic PFAS based on their functional groups and volatility. As depicted, neutral precursors predominantly exist in the gas phase due to their higher volatility and lower particle affinity. In contrast, more functionalized or ionic compounds show a stronger tendency to associate with atmospheric particles, due to their lower volatility and greater sorption potential. This spectrum captures the continuum of phase distribution, providing a conceptual overview of the behavior discussed throughout the literature based on functionalization and chain length.

The functionalization effect was observed in a study conducted in the marine atmosphere extending from the Japan Sea to the Arctic Ocean.<sup>52</sup> Fluoroalkyl sulfonamidoethanols (FASEs) possessed the highest affinity for particles, roughly 26%, followed by fluoroalkyl sulfonamides (FASAs), FTOHs, and

fluorotelomer acids (FTAs), with 1.8%.<sup>52</sup> FASEs possess the least volatility as they contain both sulfonamide and hydroxyl groups, inducing hydrogen bonding with the particulate phase.<sup>52</sup> In a study conducted in Germany, FTOHs were also found to be the most prevalent in the gas phase as they exhibit high volatility.<sup>83</sup> Similarly, the influence of the functional group on particle-associated fraction was also identified in a study of the Canadian Arctic atmosphere.<sup>20</sup> The particle-associated fraction decreased as follows: FOSEs (25%), PFOSA derivatives (9%), and FTOHs (1%),<sup>20</sup> consistent with observations by Karaskova *et al.* who reported that volatile PFOSA derivatives and FOSEs are abundant in the gas phase.<sup>160</sup> Moreover, in samples collected over the Gulf of Mexico, Shoeib *et al.* revealed that the highest particle-phase fraction was that for EtFOSE (42%), followed by 8 : 2 FTOH (26%), 10 : 2 FTOH, and MeFOSE (15%).<sup>142</sup> Ethyl-substituted compounds, NEtFOSE, NEtFOSA, also tend to exhibit higher particle association than their methyl-substituted counterparts.<sup>61</sup>

Within the FTOH homologous series, particle association generally increases with chain length, with short-chain FTOHs such as 4 : 2 and 6 : 2 occurring almost exclusively in the gas phase and longer-chain compounds such as 8 : 2 and 10 : 2 showing slightly greater particulate fraction.<sup>161</sup> Tian *et al.* proposed that as the chain length increases, stronger binding to particles is exhibited, raising the particle–air partitioning coefficient since longer chains exhibit a greater octanol–air partitioning coefficient.<sup>162</sup> This trend was also suggested by multiple other studies in current atmospheric PFAS literature.<sup>20,26,101,163,164</sup> However, ultra-short-chain PFCAs such as TFA and PFPrA may deviate from this trend because their small size and functionalization alter their partitioning behavior.<sup>162</sup> PFOSA derivatives, FOSEs, and PFDS appear to be predominantly found in the gas phase, while PFOS are strongly particle bound.<sup>165</sup> Compared to longer PFCAs, PFOA appears to exist more in the gaseous

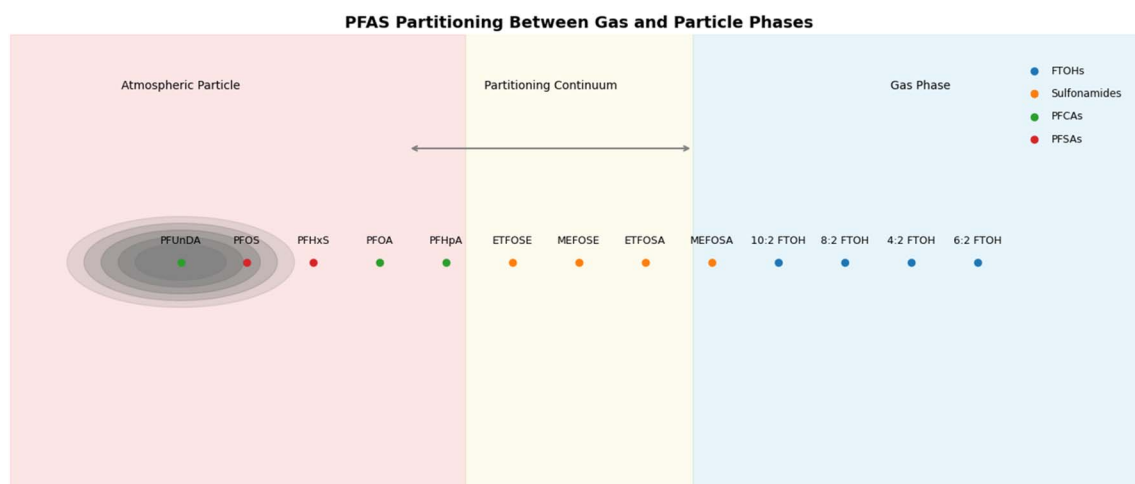
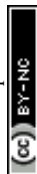


**Fig. 10** Conceptual spectrum illustrating the relative partitioning tendencies of selected PFAS between atmospheric particle and gas phases. The horizontal position represents increasing gas-phase affinity from left (strong particle association) to right (predominantly gaseous occurrence), based on compound volatility, functional group polarity, and carbon-chain length. Shaded regions denote approximate dominant phase behavior: particle associated zone (left), mixed partitioning continuum (center), gas-phase-dominated zone (right). Compounds are ordered qualitatively according to trends reported in the literature rather than quantitative partition coefficients. Colors distinguish PFAS classes (FTOHs, sulfonamides/sulfonamidoethanols, PFCAs, and PFSAs).



phase.<sup>165</sup> Similarly, PFOA and PFNA have been detected in the gas phase, revealing greater ability for LRAT.<sup>25</sup> Shorter chain PFCAs appear to be prevalent in the particulate phase, as they are well-adsorbed to mineral ions.<sup>25</sup>

When considered collectively, perfluorinated compounds (PFCs) often show greater adsorption to coarse than fine particulate matter, suggesting that coarse PM may act as an important atmospheric carrier.<sup>99</sup> However, perfluoroalkyl acids tend to associate distinctly to fine and coarse PM. PFUnDA tends to be mostly associated with fine PM due to its low volatility, whereas PFOS, PFHxS, PFHpA tend to mostly exist in coarse PM as they are more volatile than other PFAAs.<sup>166</sup> PFOA appears to exhibit a bimodal distribution as it can exist in protonated or deprotonated forms, thereby altering its sorption characteristics.<sup>166</sup> Longer chain PFCAs and FTOHs appear to associate well with fine PM,<sup>167</sup> similar to the previous finding on the association of PFUnDA with fine PM.<sup>166</sup> It was also revealed<sup>167</sup> that the sorption of 6:2 and 8:2 FTOH could be controlled by the presence of organic matter, whereas that of ionic PFAS could be related to mineral components that induce electrostatic interactions.

In addition to physicochemical properties, meteorological conditions also influence PFAS distribution and partitioning.<sup>168</sup> For example, temperature and humidity were identified as important factors affecting phase partitioning and regional distribution of PFAS.<sup>67</sup> Higher temperatures tend to increase the volatility of PFAS, increasing their occurrence in the gas phase.<sup>82</sup> For instance, 6:2 FTOH concentrations gradually increased from 9.4 pg m<sup>-3</sup> to 20 pg m<sup>-3</sup> with rising temperatures near the equator.<sup>82</sup> Temperature dependent variations were also studied by Li *et al.* revealing that short chain PFAS are highly sensitive to temperature due to their increased volatility, while long-chain PFAS are less sensitive to temperature fluctuations as they are more particle-bound.<sup>169</sup> However, another study showed that atmospheric levels of PFAS were insignificantly correlated with temperature and latitude.<sup>48</sup> This finding could be attributed to specific factors that govern the atmosphere in the study area, where long range atmospheric transport (LRAT) could play a more important role than temperature-related factors.<sup>48</sup> Remarkably, a temperature-dependent partitioning of FOSEs seems to affect their detection in the particulate phase.<sup>170</sup> FOSEs appear to have a greater particulate affinity at lower temperature than higher ones.<sup>170</sup> This could imply that higher temperatures could increase the atmospheric mobility of FOSEs. However, FTOHs and PFOSA derivatives are mostly found in the gas phase,<sup>170</sup> increasing their transport in the atmosphere and their potential degradation into more persistent PFAS. In another study, it was shown that as temperatures decreased, the partitioning of MeFOSE and EtFOSE to the particulate phase increased, but FTOH did not show any temperature dependent trend.<sup>46</sup> In regard to perfluoroalkyl acids, they appear to be most abundant in colder seasons than warmer ones.<sup>74</sup> For instance, PFOS levels were shown to be the highest in the winter and the lowest in the summer.<sup>74</sup> This could be attributed to increased volatility in the summer, increased emission sources in winter, or winter temperature inversions that could trap pollutants near the surface.<sup>74</sup>

Arp *et al.* showed that the gas/particle partitioning constant varied significantly with relative humidity for polar compounds, but not for nonpolar compounds.<sup>171</sup> This type of contrasting relative humidity dependence of partitioning between the different compounds supports the dual-phase sorption mechanism.<sup>171</sup> The water-insoluble organic matter phase, which is independent of relative humidity, strongly induces the partitioning of nonpolar compounds.<sup>171</sup> However, the polar compounds significantly partition into the mixed-aqueous phase, which depends on relative humidity.<sup>171</sup> The variation in relative humidity for ionic PFAS has also been indicated by Kim *et al.*, in which PFAAs predominate in the aqueous phase when the relative humidity exceeds 40%.<sup>172</sup> At lower relative humidity levels, the gas-phase fractions increase, with long chain PFAAs existing predominantly in that phase under drier conditions.<sup>172</sup> Much of the literature agrees that relative humidity is negatively associated with concentrations of PFAAs<sup>173,174</sup> as water molecules could slow down the oxidation of PFAAs.<sup>175</sup> However, higher PFAS concentrations have been temporarily revealed during precipitation events as liquid water droplets can act as PFAS carriers.<sup>169</sup> Following the rainfall, the levels of particle-phase PFAS decrease *via* scavenging, while an increase is observed in the concentration of gas-phase PFAS as some PFAS volatilize back into the gas phase from wet surfaces or rain droplets.<sup>169</sup>

When developing a model to represent the gas-particle partition coefficients of neutral PFAS, the sensitivity of four input parameters affecting gas deposition flux was tested, including wind speed, concentration, temperature, and Henry's law constant.<sup>176</sup> Among those four parameters, wind speed was revealed to be the most sensitive parameter for the flux with 60.9% variance for 8:2 FTOH.<sup>176</sup> Wind speed could also affect the formation and enrichment of SSA. In the Atlantic Ocean, field measurements showed that PFAAs can be enriched in SSAs by over 100 000 times compared to seawater concentrations.<sup>177</sup> Field measurements conducted in the Southern Ocean, characterized with high wind speeds, also show SSA enrichment factors between 522 and 4690.<sup>178</sup> Those findings underscore the role of wind-driven processes on PFAS partitioning.

Research on PFAS partitioning is important to understand their multiphase chemistry and interactions within different atmospheric components. Further research should focus on two key aspects that are limited in the literature. Firstly, there is a need to further investigate sorption patterns onto fine and coarse particulate matter to expand our understanding of PFAS interactions with natural and anthropogenic emissions. Secondly, more laboratory and field studies should be conducted to explore partitioning under different meteorological conditions, which could help inform atmospheric PFAS models.

## 5. Current knowledge gaps and future research

The ongoing detection of neutral PFAS in the Arctic, Antarctic, and subpolar regions underscores the importance of increased research in remote environments. However, the limited



availability of long-term atmospheric monitoring datasets in these regions constrains the ability to resolve seasonal variability, quantify long range atmospheric transport (LRAT) pathways, and assess transformation processes of volatile precursors. Expanding sustained sampling monitoring programs would therefore improve understanding of PFAS persistence and global redistribution. Midlatitude regions host the majority of industrialized zones and also act as an atmospheric transport pathway carrying PFAS toward remote areas around the world. Rapid industrialization, high population density, and the shift of fluorochemical production to China and neighboring countries make East Asia the most significant contributor to atmospheric PFAS, with concentrations far exceeding those in other regions. Nevertheless, data remain scarce across several midlatitude regions, particularly in parts of North America, limiting the accuracy of atmospheric transport modeling and regional emission inventories. The development of expanded monitoring networks and harmonized measurement approaches is therefore needed to improve spatial coverage and comparability.

In tropical and sub-tropical regions, broader atmospheric PFAS sampling in Africa, Latin America, and the Middle East is urgently needed to close geographic knowledge gaps. While certain monitored regions display low PFAS concentrations, largely influenced by local meteorological conditions, elevated levels are observed in areas with intensive industrial activity, particularly subtropical industrial hubs. This lack of data restricts understanding of PFAS cycling in high-precipitation environments, where intense wet deposition and rapid atmospheric processing may significantly influence environmental distribution. Future research should also investigate PFAS cycling in rainforests, which serve as major atmospheric sinks and biodiversity hotspots.

While ongoing progress is being made towards understanding PFAS deposition in the atmosphere, further research could investigate the role of fog in deposition and improve monitoring programs to include short-chain PFAS and replacement compounds to avoid underestimating total deposition fluxes in coastal and mountainous environments. Moreover, standardized units to report the flux such as ng per m<sup>2</sup> per day should be promoted to enable better comparability of deposition fluxes across the different regions. Finally, event-based and seasonal sampling should be incorporated rather than relying solely on long-term averages to capture the variability of deposition along with peak fluxes.

Moreover, volatile precursors such as FTOHs demonstrate sufficient lifetimes to undergo long-range atmospheric transport, ultimately degrading into more persistent PFAAs. Phase behavior is dictated by several factors including functionalization and chain length. However, the role of environmental variables, such as temperature, humidity, pressure, and aerosol composition, in shaping sorption patterns should be further investigated through modeling, controlled laboratory experiments, and fieldwork. Moreover, atmospheric transformation pathways are necessary to investigate, particularly in under-represented and remote regions, influenced by LRAT. Methods such as isotope tracking and laboratory kinetics should be

employed to tackle existing knowledge gaps regarding PFAS atmospheric lifetimes, source attribution, and re-emission processes from snowpacks and marine aerosols.

## 6. Policy and future directions

The Stockholm Protocol, the legally binding treaty designed to safeguard human health and protect the environment from persistent organic pollutants, mainly focuses on PFOA, PFOS, PFHxS, long-chain PFCAs, and other related compounds.<sup>179</sup> However, limiting regulation to a small group of end-product compounds may therefore be insufficient to control the broader spectrum of PFAS transformation products present in the environment. Therefore, this review strongly suggests that regulatory reforms should focus on both legacy and emerging compounds at international scales. Particularly, future conventions and implementations should integrate neutral PFAS, such as FTOHs, that are widely discussed in this paper, into their regulatory and monitoring policies. Regulations of PFOA and PFOS only are insufficient to control the broader spectrum of transformation products generated in the atmosphere. The transformations of those PFAS precursors have been shown to be detrimental as more persistent compounds form in various regions. Global requirements for manufacturers should be enforced to properly report and control the levels of PFAS during the use, production, and disposal processes.

Policies could tackle stricter emission control in industrial centers and enhance global agreements on the production, use, and phase-out of PFAS to protect vulnerable remote ecosystems such as the polar regions. In North America and Europe, elevated levels were detected, despite continuous restrictions, highlighting the importance of monitoring and control. It is also necessary to implement more harmonized international monitoring standards to tackle PFAS pollution in East Asian industrial centers. The current shift to short-chain PFAS is also a major issue due to their increased environmental persistence and toxicity. Consequently, governments should fund research into the toxicity and environmental fate of short-chain PFAS and phase-out their use in consumer and industrial products. In addition, routine monitoring programs should be expanded to include neutral precursors and newly introduced replacement compounds, rather than focusing only on regulated legacy PFAS. A broader class-based regulatory approach may also be needed to prevent the continued substitution of restricted PFAS with structurally similar alternatives that retain high mobility and persistence.

## Conflicts of interest

The authors declare that there are no conflicts of interest.

## Data availability

No primary research results, software, or code have been included, and no new data were generated or analyzed as part of this review.



## Acknowledgements

This work was funded by the Lebanese American University (LAU) President's Intramural Research Fund (PIRF) No. I0010.

## References

- 1 D. C. Perera and J. N. Meegoda, PFAS: The Journey from Wonder Chemicals to Environmental Nightmares and the Search for Solutions, *Appl. Sci.*, 2024, **14**, 8611.
- 2 R. C. Buck, J. Franklin, U. Berger, J. M. Conder, I. T. Cousins, P. de Voogt, A. A. Jensen, K. Kannan, S. A. Mabury and S. P. van Leeuwen, Perfluoroalkyl and polyfluoroalkyl substances in the environment: Terminology, classification, and origins, *Integr. Environ. Assess. Manag.*, 2011, **7**, 513–541.
- 3 Summary report on the new comprehensive global database of Per- and Polyfluoroalkyl Substances (PFASs), [https://www.oecd.org/en/publications/summary-report-on-the-new-comprehensive-global-database-of-per-and-polyfluoroalkyl-substances-pfass\\_1a14ad6c-en.html](https://www.oecd.org/en/publications/summary-report-on-the-new-comprehensive-global-database-of-per-and-polyfluoroalkyl-substances-pfass_1a14ad6c-en.html), accessed 12 February 2025.
- 4 Reconciling Terminology of the Universe of Per- and Polyfluoroalkyl Substances, [https://www.oecd.org/en/publications/reconciling-terminology-of-the-universe-of-per-and-polyfluoroalkyl-substances\\_e458e796-en.html](https://www.oecd.org/en/publications/reconciling-terminology-of-the-universe-of-per-and-polyfluoroalkyl-substances_e458e796-en.html), accessed 12 February 2025.
- 5 C. Hogue, US EPA broadens its definition of PFAS, *CEN J. Global Enterpren.*, 2022, **100**, 11.
- 6 E. Pasecnaja, V. Bartkevics and D. Zacs, Occurrence of selected per- and polyfluorinated alkyl substances (PFASs) in food available on the European market – A review on levels and human exposure assessment, *Chemosphere*, 2022, **287**, 132378.
- 7 Synthesis paper on per and polyfluorinated chemicals, [https://www.oecd.org/en/publications/synthesis-paper-on-per-and-polyfluorinated-chemicals\\_0bc75123-en.html](https://www.oecd.org/en/publications/synthesis-paper-on-per-and-polyfluorinated-chemicals_0bc75123-en.html), accessed 14 February 2025.
- 8 M. Forsthuber, A. M. Kaiser, S. Granitzer, I. Hassl, M. Hengstschläger, H. Stangl and C. Gundacker, Albumin is the major carrier protein for PFOS, PFOA, PFHxS, PFNA and PFDA in human plasma, *Environ. Int.*, 2020, **137**, 105324.
- 9 Y. Fujii, K. H. Harada, T. Nakamura, Y. Kato, C. Ohta, N. Koga, O. Kimura, T. Endo, A. Koizumi and K. Haraguchi, Perfluorinated carboxylic acids in edible clams: A possible exposure source of perfluorooctanoic acid for Japanese population, *Environ. Pollut.*, 2020, **263**, 114369.
- 10 C. Bach, V. Boiteux, J. Hemard, A. Colin, C. Rosin, J.-F. Munoz and X. Dauchy, Simultaneous determination of perfluoroalkyl iodides, perfluoroalkane sulfonamides, fluorotelomer alcohols, fluorotelomer iodides and fluorotelomer acrylates and methacrylates in water and sediments using solid-phase microextraction-gas chromatography/mass spectrometry, *J. Chromatogr., A*, 2016, **1448**, 98–106.
- 11 U. Eriksson, J. F. Mueller, L.-M. L. Toms, P. Hobson and A. Kärrman, Temporal trends of PFASs, PFCAs and selected precursors in Australian serum from 2002 to 2013, *Environ. Pollut.*, 2017, **220**, 168–177.
- 12 Y. Huang, M. Lu, H. Li, M. Bai and X. Huang, Sensitive determination of perfluoroalkane sulfonamides in water and urine samples by multiple monolithic fiber solid-phase microextraction and liquid chromatography tandem mass spectrometry, *Talanta*, 2019, **192**, 24–31.
- 13 M. Kreychman, E. Ivantsova, A. Lu, J. H. Bisesi and C. J. Martyniuk, A comparative review of the toxicity mechanisms of perfluorohexanoic acid (PFHxA) and perfluorohexanesulphonic acid (PFHxS) in fish, *Comp. Biochem. Physiol., Part C: Toxicol. Pharmacol.*, 2024, **279**, 109874.
- 14 M. Ateia, A. Maroli, N. Tharayil and T. Karanfil, The overlooked short- and ultrashort-chain poly- and perfluorinated substances: A review, *Chemosphere*, 2019, **220**, 866–882.
- 15 S. E. Loveless, B. Slezak, T. Serex, J. Lewis, P. Mukerji, J. C. O'Connor, E. M. Donner, S. R. Frame, S. H. Korzeniowski and R. C. Buck, Toxicological evaluation of sodium perfluorohexanoate, *Toxicology*, 2009, **264**, 32–44.
- 16 J. E. Klaunig, M. Shinohara, H. Iwai, C. P. Chengelis, J. B. Kirkpatrick, Z. Wang and R. H. Bruner, Evaluation of the chronic toxicity and carcinogenicity of perfluorohexanoic acid (PFHxA) in Sprague-Dawley rats, *Toxicol. Pathol.*, 2015, **43**, 209–220.
- 17 S. Liu, R. Yang, N. Yin and F. Faiola, The short-chain perfluorinated compounds PFBS, PFHxS, PFBA and PFHxA, disrupt human mesenchymal stem cell self-renewal and adipogenic differentiation, *J. Environ. Sci.*, 2020, **88**, 187–199.
- 18 S. J. Chow, N. Ojeda, J. G. Jacangelo and K. J. Schwab, Detection of ultrashort-chain and other per- and polyfluoroalkyl substances (PFAS) in U.S. bottled water, *Water Res.*, 2021, **201**, 117292.
- 19 L. Ahrens, W. Gerwinski, N. Theobald and R. Ebinghaus, Sources of polyfluoroalkyl compounds in the North Sea, Baltic Sea and Norwegian Sea: Evidence from their spatial distribution in surface water, *Mar. Pollut. Bull.*, 2010, **60**, 255–260.
- 20 L. Ahrens, M. Shoeib, S. D. Vento, G. Codling and C. Halsall, Polyfluoroalkyl compounds in the Canadian Arctic atmosphere, *Environ. Chem.*, 2011, **8**, 399–406.
- 21 K. Dasu, X. Xia, D. Siriwardena, T. P. Klupinski and B. Seay, Concentration profiles of per- and polyfluoroalkyl substances in major sources to the environment, *J. Environ. Manage.*, 2022, **301**, 113879.
- 22 X. Li, W. Li, Z. Wang, X. Wang, Y. Cai and Y. Shi, Atmospheric Emission of Per- and Polyfluoroalkyl Substances (PFAS) from a Fluoropolymer Manufacturing Facility: Focus on Emerging PFAS and the Potential Contribution of Condensable PFAS on their Atmospheric Partitioning, *Environ. Sci. Technol.*, 2025, **59**, 9709–9720.



- 23 R. Naidu, M. Mallavarapu, Y. Liu and A. Umeh, *Per- and Polyfluorinated Alkyl Substances: Occurrence, Toxicity and Remediation of PFAS*, Walter de Gruyter GmbH & Co KG, 2025.
- 24 B. Qiao, D. Song, B. Fang, H. Yu, X. Li, L. Zhao, Y. Yao, L. Zhu, H. Chen and H. Sun, Nontarget Screening and Fate of Emerging Per- and Polyfluoroalkyl Substances in Wastewater Treatment Plants in Tianjin, China, *Environ. Sci. Technol.*, 2023, **57**, 20127–20137.
- 25 Y. Yao, S. Chang, H. Sun, Z. Gan, H. Hu, Y. Zhao and Y. Zhang, Neutral and ionic per- and polyfluoroalkyl substances (PFASs) in atmospheric and dry deposition samples over a source region (Tianjin, China), *Environ. Pollut.*, 2016, **212**, 449–456.
- 26 N. L. Stock, V. I. Furdui, D. C. G. Muir and S. A. Mabury, Perfluoroalkyl Contaminants in the Canadian Arctic: Evidence of Atmospheric Transport and Local Contamination, *Environ. Sci. Technol.*, 2007, **41**, 3529–3536.
- 27 S. Schellenberger, I. Liagkouridis, R. Awad, S. Khan, M. Plassmann, G. Peters, J. P. Benskin and I. T. Cousins, An Outdoor Aging Study to Investigate the Release of Per- and Polyfluoroalkyl Substances (PFAS) from Functional Textiles, *Environ. Sci. Technol.*, 2022, **56**, 3471–3479.
- 28 X. Zhao, S. Zhang, Z. Hu, Z. Ren, T. Wang, B. Zhu, L. An, H. Wang and J. Liu, Research on the PFAS release and migration behavior of multi-layer outdoor jacket fabrics, *J. Hazard. Mater.*, 2025, **487**, 137218.
- 29 L. Liu, M. Lu, X. Cheng, G. Yu and J. Huang, Suspect screening and nontargeted analysis of per- and polyfluoroalkyl substances in representative fluorocarbon surfactants, aqueous film-forming foams, and impacted water in China, *Environ. Int.*, 2022, **167**, 107398.
- 30 Y. Luo, C. T. Gibson, C. Chuah, Y. Tang, R. Naidu and C. Fang, Raman imaging for the identification of Teflon microplastics and nanoplastics released from non-stick cookware, *Sci. Total Environ.*, 2022, **851**, 158293.
- 31 S. Namazkar, O. Ragnarsdottir, A. Josefsson, F. Branzell, S. Abel, M. A.-E. Abdallah, S. Harrad and J. P. Benskin, Characterization and dermal bioaccessibility of residual- and listed PFAS ingredients in cosmetic products, *Environ. Sci. Process. Impacts*, 2024, **26**, 259–268.
- 32 K. T. Eriksen, O. Raaschou-Nielsen, J. K. McLaughlin, L. Lipworth, A. Tjønneland, K. Overvad and M. Sørensen, Association between plasma PFOA and PFOS levels and total cholesterol in a middle-aged Danish population, *PLoS One*, 2013, **8**, e56969.
- 33 E. Panieri, K. Baralic, D. Djukic-Cosic, A. Buha Djordjevic and L. Saso, PFAS Molecules: A Major Concern for the Human Health and the Environment, *Toxics*, 2022, **10**, 44.
- 34 A. Conti, C. Strazzeri and K. J. Rhoden, Perfluorooctane sulfonic acid, a persistent organic pollutant, inhibits iodide accumulation by thyroid follicular cells in vitro, *Mol. Cell. Endocrinol.*, 2020, **515**, 110922.
- 35 C. Freire, F. Vela-Soria, F. Castiello, E. Salamanca-Fernández, R. Quesada-Jiménez, M. C. López-Alados, M. F. Fernandez and N. Olea, Exposure to perfluoroalkyl substances (PFAS) and association with thyroid hormones in adolescent males, *Int. J. Hyg Environ. Health*, 2023, **252**, 114219.
- 36 A. Rodríguez-Carrillo, E. Salamanca-Fernández, E. den Hond, V. J. Verheyen, L. Fábelová, L. P. Murinova, S. Pedraza-Díaz, A. Castaño, J. V. García-Lario, S. Remy, E. Govarts, G. Schoeters, N. Olea, C. Freire and M. F. Fernández, Association of exposure to perfluoroalkyl substances (PFAS) and phthalates with thyroid hormones in adolescents from HBM4EU aligned studies, *Environ. Res.*, 2023, **237**, 116897.
- 37 K. Abraham, H. Mielke, H. Fromme, W. Völkel, J. Menzel, M. Peiser, F. Zepp, S. N. Willich and C. Weikert, Internal exposure to perfluoroalkyl substances (PFASs) and biological markers in 101 healthy 1-year-old children: associations between levels of perfluorooctanoic acid (PFOA) and vaccine response, *Arch. Toxicol.*, 2020, **94**, 2131–2147.
- 38 P. Grandjean, C. Heilmann, P. Weihe, F. Nielsen, U. B. Mogensen and E. Budtz-Jørgensen, Serum Vaccine Antibody Concentrations in Adolescents Exposed to Perfluorinated Compounds, *Environ. Health Perspect.*, 2017, **125**, 077018.
- 39 M. Haug, L. Dunder, P. M. Lind, L. Lind and S. Salihovic, Associations of perfluoroalkyl substances (PFAS) with lipid and lipoprotein profiles, *J. Expo. Sci. Environ. Epidemiol.*, 2023, **33**, 757–765.
- 40 X. Cheng, Y. Wei, Z. Zhang, F. Wang, J. He, R. Wang, Y. Xu, M. Keerman, S. Zhang, Y. Zhang, J. Bi, J. Yao and M. He, Plasma PFOA and PFOS Levels, DNA Methylation, and Blood Lipid Levels: A Pilot Study, *Environ. Sci. Technol.*, 2022, **56**, 17039–17051.
- 41 IARC Monographs Volume 135: Perfluorooctanoic acid (PFOA) and perfluorooctanesulfonic acid (PFOS) – IARC, <https://www.iarc.who.int/news-events/iarc-monographs-volume-135-perfluorooctanoic-acid-pfoa-and-perfluorooctanesulfonic-acid-pfos/>, accessed 2 June 2025.
- 42 A. Winquist, J. M. Hodge, W. R. Diver, J. L. Rodriguez, A. N. Troeschel, J. Daniel and L. R. Teras, Case-Cohort Study of the Association between PFAS and Selected Cancers among Participants in the American Cancer Society's Cancer Prevention Study II LifeLink Cohort, *Environ. Health Perspect.*, 2023, **131**, 127007.
- 43 M. S. Seyyedsalehi and P. Boffetta, Per- and Poly-fluoroalkyl Substances (PFAS) Exposure and Risk of Kidney, Liver, and Testicular Cancers: A Systematic Review and Meta-Analysis, *Med. Lav.*, 2023, **114**, e2023040.
- 44 P. C. Obiako, S. O. Ayisire and C. M. Sayes, Impact of perfluorooctanoic acid (PFOA) and perfluorobutanoic acid (PFBA) on oxidative stress and metabolic biomarkers in human neuronal cells (SH-SY5Y), *Environ. Int.*, 2024, **190**, 108864.
- 45 J. M. Goodrich, M. M. Calkins, A. J. Caban-Martinez, T. Stueckle, C. Grant, A. M. Calafat, A. Nematollahi, A. M. Jung, J. M. Graber, T. Jenkins, A. L. Slitt, A. Dewald, J. Cook Botelho, S. Beitel, S. Littau, J. Gulotta, D. Wallentine, J. Hughes, C. Popp and J. L. Burgess, Per- and Polyfluoroalkyl Substances, Epigenetic Age and DNA



- Methylation: A Cross-Sectional Study of Firefighters, *Epigenomics*, 2021, **13**, 1619–1636.
- 46 M. Shoeib, T. Harner and P. Vlahos, Perfluorinated chemicals in the arctic atmosphere, *Environ. Sci. Technol.*, 2006, **40**, 7577–7583.
- 47 Weird Science: Polar Circles and Tropical Circles|[manoa.hawaii.edu/ExploringOurFluidEarth](http://manoa.hawaii.edu/ExploringOurFluidEarth), <https://manoa.hawaii.edu/exploringourfluidearth/physical/world-ocean/locating-points-globe/weird-science-polar-circles-and-tropical-circles>, accessed 21 May 2025.
- 48 Z. Wang, Z. Xie, W. Mi, A. Möller, H. Wolschke and R. Ebinghaus, Neutral Poly/Per-Fluoroalkyl Substances in Air from the Atlantic to the Southern Ocean and in Antarctic Snow, *Environ. Sci. Technol.*, 2015, **49**, 7770–7775.
- 49 Z. Xie, Z. Wang, W. Mi, A. Möller, H. Wolschke and R. Ebinghaus, Neutral Poly-/perfluoroalkyl Substances in Air and Snow from the Arctic, *Sci. Rep.*, 2015, **5**, 8912.
- 50 S. D. Vento, C. Halsall, R. Gioia, K. Jones and J. Dachs, Volatile per- and polyfluoroalkyl compounds in the remote atmosphere of the western Antarctic Peninsula: an indirect source of perfluoroalkyl acids to Antarctic waters?, *Atmos. Pollut. Res.*, 2012, **3**, 450–455.
- 51 Draft state of per- and polyfluoroalkyl substances (PFAS) report, <https://www.canada.ca/en/environment-climate-change/services/evaluating-existing-substances/draft-state-per-polyfluoroalkyl-substances-report.html>, accessed 20 May 2025.
- 52 M. Cai, Z. Xie, A. Möller, Z. Yin, P. Huang, M. Cai, H. Yang, R. Sturm, J. He and R. Ebinghaus, Polyfluorinated compounds in the atmosphere along a cruise pathway from the Japan Sea to the Arctic Ocean, *Chemosphere*, 2012, **87**, 989–997.
- 53 R. Bossi, K. Vorkamp and H. Skov, Concentrations of organochlorine pesticides, polybrominated diphenyl ethers and perfluorinated compounds in the atmosphere of North Greenland, *Environ. Pollut.*, 2016, **217**, 4–10.
- 54 S. Genualdi, S. C. Lee, M. Shoeib, A. Gawor, L. Ahrens and T. Harner, Global pilot study of legacy and emerging persistent organic pollutants using sorbent-impregnated polyurethane foam disk passive air samplers, *Environ. Sci. Technol.*, 2010, **44**, 5534–5539.
- 55 J. P. Giesy and K. Kannan, Global Distribution of Perfluorooctane Sulfonate in Wildlife, *Environ. Sci. Technol.*, 2001, **35**, 1339–1342.
- 56 E. D. Goldberg, Synthetic organohalides in the sea, *Proc. R. Soc. Lond. B Biol. Sci.*, 1975, **189**, 277–289.
- 57 F. Rubel and M. Kottke, Observed and projected climate shifts 1901–2100 depicted by world maps of the Köppen-Geiger climate classification, *Meteorol. Z.*, 2010, 135–141.
- 58 R. G. Bailey, in *Ecoregions: the Ecosystem Geography of the Oceans and Continents*, ed. R. G. Bailey, Springer, New York, NY, 2014, pp. 55–68.
- 59 L. G. T. Gaines, Historical and current usage of per- and polyfluoroalkyl substances (PFAS): A literature review, *Am. J. Ind. Med.*, 2023, **66**, 353–378.
- 60 X. Wang, J. Schuster, K. C. Jones and P. Gong, Occurrence and spatial distribution of neutral perfluoroalkyl substances and cyclic volatile methylsiloxanes in the atmosphere of the Tibetan Plateau, *Atmos. Chem. Phys.*, 2018, **18**, 8745–8755.
- 61 J. L. Barber, U. Berger, C. Chaemfa, S. Huber, A. Jahnke, C. Temme and K. C. Jones, Analysis of per- and polyfluorinated alkyl substances in air samples from Northwest Europe, *J. Environ. Monit.*, 2007, **9**, 530–541.
- 62 G.-H. Seo, Y.-K. Cho and B.-J. Choi, Variations of heat transport in the northwestern Pacific marginal seas inferred from high-resolution reanalysis, *Prog. Oceanogr.*, 2014, **121**, 98–108.
- 63 X. Yin, S. Kang, M. Rupakheti, B. de Foy, P. Li, J. Yang, K. Wu, Q. Zhang and D. Rupakheti, Influence of transboundary air pollution on air quality in southwestern China, *Geosci. Front.*, 2021, **12**, 101239.
- 64 K.-I. Chang, W. J. Teague, S. J. Lyu, H. T. Perkins, D.-K. Lee, D. R. Watts, Y.-B. Kim, D. A. Mitchell, C. M. Lee and K. Kim, Circulation and currents in the southwestern East/Japan Sea: Overview and review, *Prog. Oceanogr.*, 2004, **61**, 105–156.
- 65 H. Kasai, H. Saito, A. Yoshimori and S. Taguchi, Variability in timing and magnitude of spring bloom in the Oyashio region, the western subarctic Pacific off Hokkaido, Japan, *Fish. Oceanogr.*, 1997, **6**, 118–129.
- 66 S. Wang, X. Lin, Q. Li, C. Liu, Y. Li and X. Wang, Neutral and ionizable per-and polyfluoroalkyl substances in the urban atmosphere: Occurrence, sources and transport, *Sci. Total Environ.*, 2022, **823**, 153794.
- 67 X. Fang, Q. Wang, Z. Zhao, J. Tang, C. Tian, Y. Yao, J. Yu and H. Sun, Distribution and dry deposition of alternative and legacy perfluoroalkyl and polyfluoroalkyl substances in the air above the Bohai and Yellow Seas, China, *Atmos. Environ.*, 2018, **192**, 128–135.
- 68 B. Wang, *The Asian Monsoon*, Springer Science & Business Media, 2006.
- 69 Ryukyu Islands|Japan, Map, History, World War II, & Location|Britannica, <https://www.britannica.com/place/Ryukyu-Islands>, accessed 2 June 2025.
- 70 A. L, The Evolution of the East Asian Eco-Developmental State, <https://apjif.org/2021/6/haddad-harrell>, accessed 2 June 2025.
- 71 X. Du, R. Chen and H. Kan, Challenges of Air Pollution and Health in East Asia, *Curr. Environ. Health Rep.*, 2024, **11**, 89–101.
- 72 C. Chen, Y. Lu, X. Zhang, J. Geng, T. Wang, Y. Shi, W. Hu and J. Li, A review of spatial and temporal assessment of PFOS and PFOA contamination in China, *Chem. Ecol.*, 2009, **25**, 163–177.
- 73 S.-K. Kim, M. Shoeib, K.-S. Kim and J.-E. Park, Indoor and outdoor poly- and perfluoroalkyl substances (PFASs) in Korea determined by passive air sampler, *Environ. Pollut.*, 2012, **162**, 144–150.
- 74 D. Han, Y. Ma, C. Huang, X. Zhang, H. Xu, Y. Zhou, S. Liang, X. Chen, X. Huang, H. Liao, S. Fu, X. Hu and J. Cheng, Occurrence and source apportionment of perfluoroalkyl acids (PFAAs) in the atmosphere in China, *Atmos. Chem. Phys.*, 2019, **19**, 14107–14117.



- 75 Y. He, Per- and polyfluoroalkyl Substances (PFAS) In China's Groundwater Resources: Concentration, Composition, and Human Health Risk, *E3S Web Conf.*, 2023, **406**, 02047.
- 76 Overview, <https://chm.pops.int/Implementation/IndustrialPOPs/PFAS/Overview/tabid/5221/Default.aspx#>, accessed 2 June 2025.
- 77 T. Wang, Y. Lu, C. Chen, J. E. Naile, J. S. Khim and J. P. Giesy, Perfluorinated compounds in a coastal industrial area of Tianjin, China, *Environ. Geochem. Health*, 2012, **34**, 301–311.
- 78 Y. Yao, S. Chang, Y. Zhao, J. Tang, H. Sun and Z. Xie, Per- and poly-fluoroalkyl substances (PFASs) in the urban, industrial, and background atmosphere of Northeastern China coast around the Bohai Sea: Occurrence, partitioning, and seasonal variation, *Atmos. Environ.*, 2017, **167**, 150–158.
- 79 H. Chen, Y. Yao, Z. Zhao, Y. Wang, Q. Wang, C. Ren, B. Wang, H. Sun, A. C. Alder and K. Kannan, Multimedia Distribution and Transfer of Per- and Polyfluoroalkyl Substances (PFASs) Surrounding Two Fluorochemical Manufacturing Facilities in Fuxin, China, *Environ. Sci. Technol.*, 2018, **52**, 8263–8271.
- 80 K.-C. Emeis, J. van Beusekom, U. Callies, R. Ebinghaus, A. Kannan, G. Kraus, I. Kröncke, H. Lenhart, I. Lorkowski, V. Matthias, C. Möllmann, J. Pätsch, M. Scharfe, H. Thomas, R. Weisse and E. Zorita, The North Sea — A shelf sea in the Anthropocene, *J. Mar. Syst.*, 2015, **141**, 18–33.
- 81 F. O. Heukamp, L. Aue, Q. Wang, M. Ionita, T. Kanzow, C. Wekerle and A. Rinke, Cyclones modulate the control of the North Atlantic Oscillation on transports into the Barents Sea, *Commun. Earth Environ.*, 2023, **4**, 1–11.
- 82 A. Jahnke, U. Berger, R. Ebinghaus and C. Temme, Latitudinal Gradient of Airborne Polyfluorinated Alkyl Substances in the Marine Atmosphere between Germany and South Africa (53°N–33°S), *Environ. Sci. Technol.*, 2007, **41**, 3055–3061.
- 83 A. Dreyer and R. Ebinghaus, Polyfluorinated compounds in ambient air from ship- and land-based measurements in northern Germany, *Atmos. Environ.*, 2009, **43**, 1527–1535.
- 84 Z. Xie, Z. Zhao, A. Möller, H. Wolschke, L. Ahrens, R. Sturm and R. Ebinghaus, Neutral poly- and perfluoroalkyl substances in air and seawater of the North Sea, *Environ. Sci. Pollut. Res.*, 2013, **20**, 7988–8000.
- 85 C. E. Müller, A. C. Gerecke, C. Bogdal, Z. Wang, M. Scheringer and K. Hungerbühler, Atmospheric fate of poly- and perfluorinated alkyl substances (PFASs): I. Day-night patterns of air concentrations in summer in Zurich, Switzerland, *Environ. Pollut.*, 2012, **169**, 196–203.
- 86 C. Rauert, M. Shoieb, J. K. Schuster, A. Eng and T. Harner, Atmospheric concentrations and trends of poly- and perfluoroalkyl substances (PFAS) and volatile methyl siloxanes (VMS) over 7 years of sampling in the Global Atmospheric Passive Sampling (GAPS) network, *Environ. Pollut.*, 2018, **238**, 94–102.
- 87 Z. Wang, Z. Xie, A. Möller, W. Mi, H. Wolschke and R. Ebinghaus, Atmospheric concentrations and gas/particle partitioning of neutral poly- and perfluoroalkyl substances in northern German coast, *Atmos. Environ.*, 2014, **95**, 207–213.
- 88 A. Jahnke, L. Ahrens, R. Ebinghaus and C. Temme, Urban versus Remote Air Concentrations of Fluorotelomer Alcohols and Other Polyfluorinated Alkyl Substances in Germany, *Environ. Sci. Technol.*, 2007, **41**, 745–752.
- 89 R. Harris, in *International Encyclopedia of Human Geography*, ed. R. Kitchin and N. Thrift, Elsevier, Oxford, 2009, pp. 383–388.
- 90 N. M. Brennan, A. T. Evans, M. K. Fritz, S. A. Peak and H. E. von Holst, Trends in the Regulation of Per- and Polyfluoroalkyl Substances (PFAS): A Scoping Review, *Int. J. Environ. Res. Publ. Health*, 2021, **18**, 10900.
- 91 E. Goosey and S. Harrad, Perfluoroalkyl substances in UK indoor and outdoor air: Spatial and seasonal variation, and implications for human exposure, *Environ. Int.*, 2012, **45**, 86–90.
- 92 T. J. Wallington, M. D. Hurley, J. Xia, D. J. Wuebbles, S. Sillman, A. Ito, J. E. Penner, D. A. Ellis, J. Martin, S. A. Mabury, O. J. Nielsen and M. P. Sulbaek Andersen, Formation of C7F15COOH (PFOA) and Other Perfluorocarboxylic Acids during the Atmospheric Oxidation of 8:2 Fluorotelomer Alcohol, *Environ. Sci. Technol.*, 2006, **40**, 924–930.
- 93 S.-K. Kim and K. Kannan, Perfluorinated Acids in Air, Rain, Snow, Surface Runoff, and Lakes: Relative Importance of Pathways to Contamination of Urban Lakes, *Environ. Sci. Technol.*, 2007, **41**, 8328–8334.
- 94 C. Xia, S. L. Capozzi, K. A. Romanak, D. C. Lehman, A. Dove, V. Richardson, T. Greenberg, D. McGoldrick and M. Venier, The Ins and Outs of Per- and Polyfluoroalkyl Substances in the Great Lakes: The Role of Atmospheric Deposition, *Environ. Sci. Technol.*, 2024, **58**, 9303–9313.
- 95 J. Henry, in *Encyclopedia of World Climatology*, Springer, Dordrecht, 2005, pp. 742–750.
- 96 Z. Lu, R. Lu, H. Zheng, J. Yan, L. Song, J. Wang, H. Yang and M. Cai, Risk exposure assessment of per- and polyfluoroalkyl substances (PFASs) in drinking water and atmosphere in central eastern China, *Environ. Sci. Pollut. Res.*, 2018, **25**, 9311–9320.
- 97 Y. Harb, A. Mcheik and N. Hayeck, in *Urban and Regional Air Quality*, World scientific, 2025, vol. 4, pp. 41–106.
- 98 SE Asia territories becoming global manufacturing hubs, <https://www.insidelogistics.ca/opinions/se-asia-territories-becoming-global-manufacturing-hubs/>, accessed 7 June 2025.
- 99 B. Liu, H. Zhang, D. Yao, J. Li, L. Xie, X. Wang, Y. Wang, G. Liu and B. Yang, Perfluorinated compounds (PFCs) in the atmosphere of Shenzhen, China: Spatial distribution, sources and health risk assessment, *Chemosphere*, 2015, **138**, 511–518.
- 100 J. Hu, H. Kawamura, H. Hong and Y. Qi, A Review on the Currents in the South China Sea: Seasonal Circulation,



- South China Sea Warm Current and Kuroshio Intrusion, *J. Oceanogr.*, 2000, **56**, 607–624.
- 101 E. Yamazaki, S. Taniyasu, X. Wang and N. Yamashita, Per- and polyfluoroalkyl substances in surface water, gas and particle in open ocean and coastal environment, *Chemosphere*, 2021, **272**, 129869.
- 102 S. Lai, J. Song, T. Song, Z. Huang, Y. Zhang, Y. Zhao, G. Liu, J. Zheng, W. Mi, J. Tang, S. Zou, R. Ebinghaus and Z. Xie, Neutral polyfluoroalkyl substances in the atmosphere over the northern South China Sea, *Environ. Pollut.*, 2016, **214**, 449–455.
- 103 Alongside the railroad of the biggest iron ore mine in the world: poverty, pollution, deaths and human rights violations – Observatório da Mineração, [https://observatoriodamineracao.com.br/alongside-the-railroad-of-the-biggest-iron-ore-mine-in-the-world-poverty-pollution-deaths-and-human-rights-violations/?utm\\_source=chatgpt.com](https://observatoriodamineracao.com.br/alongside-the-railroad-of-the-biggest-iron-ore-mine-in-the-world-poverty-pollution-deaths-and-human-rights-violations/?utm_source=chatgpt.com), accessed 7 June 2025.
- 104 FIEMA, <https://www.fiema.org.br/pagina/32/invest-in-maranhao#>, accessed 7 June 2025.
- 105 2.1.5 Brazil Port of Itaquí|Digital Logistics Capacity Assessments, <https://lca.logcluster.org/215-brazil-port-itaqui>, accessed 7 June 2025.
- 106 A. Saini, S. Chinnadurai, J. K. Schuster, A. Eng and T. Harner, Per- and polyfluoroalkyl substances and volatile methyl siloxanes in global air: Spatial and temporal trends, *Environ. Pollut.*, 2023, **323**, 121291.
- 107 I. Kourtchev, B. G. Sebben, A. Bogush, A. F. L. Godoi and R. H. M. Godoi, Per- and polyfluoroalkyl substances (PFASs) in urban PM<sub>2.5</sub> samples from Curitiba, Brazil, *Atmos. Environ.*, 2023, **309**, 119911.
- 108 I. Kourtchev, B. G. Sebben, S. Brill, C. Barbosa G. G., B. Weber, R. R. Ferreira, F. A. F. D'Oliveira, C. Q. Dias-Junior, O. A. M. Popoola, J. Williams, C. Pöhlker and R. H. M. Godoi, Occurrence of a “forever chemical” in the atmosphere above pristine Amazon Forest, *Sci. Total Environ.*, 2024, **944**, 173918.
- 109 Y. Wang and K. D. Good, Microplastics and PFAS air-water interaction and deposition, *Sci. Total Environ.*, 2024, **954**, 176247.
- 110 W. F. Hartz, M. K. Björnsdotter, L. W. Y. Yeung, A. Hodson, E. R. Thomas, J. D. Humby, C. Day, I. E. Jogsten, A. Kärman and R. Kallenborn, Levels and distribution profiles of Per- and Polyfluoroalkyl Substances (PFAS) in a high Arctic Svalbard ice core, *Sci. Total Environ.*, 2023, **871**, 161830.
- 111 M. K. Alam and A. Farid, *Coupled PFAS Transport and Seepage Models to Evaluate Retardation due to Air–Water–Interface Adsorption*, 2025, pp. 24–33.
- 112 H. R. Pruppacher, J. D. Klett and P. K. Wang, Microphysics of Clouds and Precipitation, *Aerosol Sci. Technol.*, 1998, **28**, 381–382.
- 113 B. Croft, R. V. Martin, W. R. Leitch, P. Tunved, T. J. Breider, S. D. D'Andrea and J. R. Pierce, Processes controlling the annual cycle of Arctic aerosol number and size distributions, *Atmos. Chem. Phys.*, 2016, **16**, 3665–3682.
- 114 E. Holopainen, H. Kokkola, A. Laakso and T. Kühn, In-cloud scavenging scheme for sectional aerosol modules – implementation in the framework of the Sectional Aerosol module for Large Scale Applications version 2.0 (SALSA2.0) global aerosol module, *Geosci. Model Dev.*, 2020, **13**, 6215–6235.
- 115 D. M. Chate, P. Murugavel, K. Ali, S. Tiwari and G. Beig, Below-cloud rain scavenging of atmospheric aerosols for aerosol deposition models, *Atmos. Res.*, 2011, **99**, 528–536.
- 116 P. Casal, Y. Zhang, J. W. Martin, M. Pizarro, B. Jiménez and J. Dachs, Role of Snow Deposition of Perfluoroalkylated Substances at Coastal Livingston Island (Maritime Antarctica), *Environ. Sci. Technol.*, 2017, **51**, 8460–8470.
- 117 W. F. Hartz, M. K. Björnsdotter, L. W. Y. Yeung, J. D. Humby, S. Eckhardt, N. Evangelidou, I. Ericson Jogsten, A. Kärman and R. Kallenborn, Sources and Seasonal Variations of Per- and Polyfluoroalkyl Substances (PFAS) in Surface Snow in the Arctic, *Environ. Sci. Technol.*, 2024, **58**, 21817–21828.
- 118 Y. D. Lei and F. Wania, Is rain or snow a more efficient scavenger of organic chemicals?, *Atmos. Environ.*, 2004, **38**, 3557–3571.
- 119 W. Zhang, L. Ma, J. Yu, C. Bu, Y. Wang, H. Zeng and Y. Han, Soil-air exchange of substituted chlorobenzenes and volatile PFAS at contaminated sites: Impact of environmental factors and development of a fugacity-based model, *J. Hazard. Mater.*, 2025, **498**, 139995.
- 120 5 Environmental Fate and Transport Processes – PFAS – Per- and Polyfluoroalkyl Substances, [https://pfas-1.itrcweb.org/5-environmental-fate-and-transport-processes/?utm\\_source=chatgpt.com](https://pfas-1.itrcweb.org/5-environmental-fate-and-transport-processes/?utm_source=chatgpt.com), accessed 15 July 2025.
- 121 J. H. Johansson, M. E. Salter, J. C. A. Navarro, C. Leck, E. D. Nilsson and I. T. Cousins, Global transport of perfluoroalkyl acids via sea spray aerosol, *Environ. Sci. Process. Impacts*, 2019, **21**, 635–649.
- 122 J. Garnett, C. Halsall, H. Winton, H. Joerss, R. Mulvaney, R. Ebinghaus, M. Frey, A. Jones, A. Leeson and P. Wynn, Increasing Accumulation of Perfluorocarboxylate Contaminants Revealed in an Antarctic Firn Core (1958–2017), *Environ. Sci. Technol.*, 2022, **56**, 11246–11255.
- 123 S. Taniyasu, N. Yamashita, H.-B. Moon, K. Y. Kwok, P. K. S. Lam, Y. Horii, G. Petrick and K. Kannan, Does wet precipitation represent local and regional atmospheric transportation by perfluorinated alkyl substances?, *Environ. Int.*, 2013, **55**, 25–32.
- 124 M. S. Shimizu, R. Mott, A. Potter, J. Zhou, K. Baumann, J. D. Surratt, B. Turpin, G. B. Avery, J. Harfmann, R. J. Kieber, R. N. Mead, S. A. Skrabal and J. D. Willey, Atmospheric Deposition and Annual Flux of Legacy Perfluoroalkyl Substances and Replacement Perfluoroalkyl Ether Carboxylic Acids in Wilmington, NC, USA, *Environ. Sci. Technol. Lett.*, 2021, **8**, 366–372.
- 125 D. Pfothner, E. Sellers, M. Olson, K. Praedel and M. Shafer, PFAS concentrations and deposition in precipitation: An intensive 5-month study at National Atmospheric Deposition Program – National trends sites (NADP-NTN) across Wisconsin, USA, *Atmos. Environ.*, 2022, **291**, 119368.



- 126 A. Dreyer, V. Matthias, I. Weinberg and R. Ebinghaus, Wet deposition of poly- and perfluorinated compounds in Northern Germany, *Environ. Pollut.*, 2010, **158**, 1221–1227.
- 127 S. Wang, X. Lin, Q. Li, Y. Li, E. Yamazaki, N. Yamashita and X. Wang, Particle size distribution, wet deposition and scavenging effect of per- and polyfluoroalkyl substances (PFASs) in the atmosphere from a subtropical city of China, *Sci. Total Environ.*, 2022, **823**, 153528.
- 128 F. Wang, W. Wang, D. Zhao, J. Liu, P. Lu, N. L. Rose and G. Zhang, Source apportionment and wet deposition of atmospheric poly- and per-fluoroalkyl substances in a metropolitan city centre of southwest China, *Atmos. Environ.*, 2022, **273**, 118983.
- 129 J. J. MacInnis, K. French, D. C. G. Muir, C. Spencer, A. Criscitiello, A. O. D. Silva and C. J. Young, Emerging investigator series: a 14-year depositional ice record of perfluoroalkyl substances in the High Arctic, *Environ. Sci. Process. Impacts*, 2017, **19**, 22–30.
- 130 C. J. Young, V. I. Furdui, J. Franklin, R. M. Koerner, D. C. G. Muir and S. A. Mabury, Perfluorinated Acids in Arctic Snow: New Evidence for Atmospheric Formation, *Environ. Sci. Technol.*, 2007, **41**, 3455–3461.
- 131 O. US EPA, TSCA Section 8(a)(7) Reporting and Recordkeeping Requirements for Perfluoroalkyl and Polyfluoroalkyl Substances, <https://www.epa.gov/assessing-and-managing-chemicals-under-tsca/tsca-section-8a7-reporting-and-recordkeeping>, accessed 21 July 2025.
- 132 O. US EPA, PFAS Strategic Roadmap, <https://www.epa.gov/pfas/pfas-strategic-roadmap-epas-commitments-action-2021-2024>, accessed 21 July 2025.
- 133 Overview, <https://chm.pops.int/implementation/industrialpops/pfos/overview/tabid/5221/default.aspx>, accessed 21 July 2025.
- 134 H. M. Pickard, A. S. Criscitiello, C. Spencer, M. J. Sharp, D. C. G. Muir, A. O. De Silva and C. J. Young, Continuous non-marine inputs of per- and polyfluoroalkyl substances to the High Arctic: a multi-decadal temporal record, *Atmos. Chem. Phys.*, 2018, **18**, 5045–5058.
- 135 X. Wang, M. Chen, P. Gong and C. Wang, Perfluorinated alkyl substances in snow as an atmospheric tracer for tracking the interactions between westerly winds and the Indian Monsoon over western China, *Environ. Int.*, 2019, **124**, 294–301.
- 136 K. R. Miner, H. Clifford, T. Taruscio, M. Potocki, G. Solomon, M. Ritari, I. E. Napper, A. P. Gajurel and P. A. Mayewski, Deposition of PFAS ‘forever chemicals’ on Mt. Everest, *Sci. Total Environ.*, 2021, **759**, 144421.
- 137 T. Kirchgeorg, A. Dreyer, J. Gabrieli, N. Kehrwald, M. Sigl, M. Schwikowski, C. Boutron, A. Gambaro, C. Barbante and R. Ebinghaus, Temporal variations of perfluoroalkyl substances and polybrominated diphenyl ethers in alpine snow, *Environ. Pollut.*, 2013, **178**, 367–374.
- 138 B. Sha, J. H. Johansson, P. Tunved, P. Bohlin-Nizzetto, I. T. Cousins and M. E. Salter, Sea Spray Aerosol (SSA) as a Source of Perfluoroalkyl Acids (PFAAs) to the Atmosphere: Field Evidence from Long-Term Air Monitoring, *Environ. Sci. Technol.*, 2022, **56**, 228–238.
- 139 M. Filipovic, H. Laudon, M. S. McLachlan and U. Berger, Mass Balance of Perfluorinated Alkyl Acids in a Pristine Boreal Catchment, *Environ. Sci. Technol.*, 2015, **49**, 12127–12135.
- 140 G. Codling, C. Halsall, L. Ahrens, S. Del Vento, K. Wiberg, M. Bergknut, H. Laudon and R. Ebinghaus, The fate of per- and polyfluoroalkyl substances within a melting snowpack of a boreal forest, *Environ. Pollut.*, 2014, **191**, 190–198.
- 141 G. Codling, A. Vogt, P. D. Jones, T. Wang, P. Wang, Y.-L. Lu, M. Corcoran, S. Bonina, A. Li, N. C. Sturchio, K. J. Rockne, K. Ji, J.-S. Khim, J. E. Naile and J. P. Giesy, Historical trends of inorganic and organic fluorine in sediments of Lake Michigan, *Chemosphere*, 2014, **114**, 203–209.
- 142 M. Shoeib, P. Vlahos, T. Harner, A. Peters, M. Graustein and J. Narayan, Survey of polyfluorinated chemicals (PFCs) in the atmosphere over the northeast Atlantic Ocean, *Atmos. Environ.*, 2010, **44**, 2887–2893.
- 143 D. A. Jackson, T. J. Wallington and S. A. Mabury, Atmospheric oxidation of polyfluorinated amides: historical source of perfluorinated carboxylic acids to the environment, *Environ. Sci. Technol.*, 2013, **47**, 4317–4324.
- 144 D. A. Ellis, J. W. Martin, S. A. Mabury, M. D. Hurley, M. P. Sulbaek Andersen and T. J. Wallington, Atmospheric Lifetime of Fluorotelomer Alcohols, *Environ. Sci. Technol.*, 2003, **37**, 3816–3820.
- 145 M. D. Hurley, J. C. Ball, T. J. Wallington, M. P. Sulbaek Andersen, D. A. Ellis, J. W. Martin and S. A. Mabury, Atmospheric Chemistry of 4:2 Fluorotelomer Alcohol (CF<sub>3</sub>(CF<sub>2</sub>)<sub>3</sub>CH<sub>2</sub>CH<sub>2</sub>OH): Products and Mechanism of Cl Atom Initiated Oxidation, *J. Phys. Chem. A*, 2004, **108**, 5635–5642.
- 146 M. D. Hurley, T. J. Wallington, M. P. Sulbaek Andersen, D. A. Ellis, J. W. Martin and S. A. Mabury, Atmospheric Chemistry of Fluorinated Alcohols: Reaction with Cl Atoms and OH Radicals and Atmospheric Lifetimes, *J. Phys. Chem. A*, 2004, **108**, 1973–1979.
- 147 M. P. Sulbaek Andersen, O. J. Nielsen, M. D. Hurley, J. C. Ball, T. J. Wallington, D. A. Ellis, J. W. Martin and S. A. Mabury, Atmospheric Chemistry of 4:2 Fluorotelomer Alcohol (n-C<sub>4</sub>F<sub>9</sub>CH<sub>2</sub>CH<sub>2</sub>OH): Products and Mechanism of Cl Atom Initiated Oxidation in the Presence of NO<sub>x</sub>, *J. Phys. Chem. A*, 2005, **109**, 1849–1856.
- 148 M. S. Chiappero, G. A. Argüello, M. D. Hurley and T. J. Wallington, Atmospheric chemistry of C<sub>8</sub>F<sub>17</sub>CH<sub>2</sub>CHO: Yield from C<sub>8</sub>F<sub>17</sub>CH<sub>2</sub>CH<sub>2</sub>OH (8:2 FTOH) oxidation, kinetics and mechanisms of reactions with Cl atoms and OH radicals, *Chem. Phys. Lett.*, 2008, **461**, 198–202.
- 149 G. Solognac, A. Mellouki, G. Le Bras, I. Barnes and Th. Benter, Reaction of Cl Atoms with C<sub>6</sub>F<sub>13</sub>CH<sub>2</sub>OH, C<sub>6</sub>F<sub>13</sub>CHO, and C<sub>3</sub>F<sub>7</sub>CHO, *J. Phys. Chem. A*, 2006, **110**, 4450–4457.
- 150 D. A. Ellis, J. W. Martin, A. O. De Silva, S. A. Mabury, M. D. Hurley, M. P. Sulbaek Andersen and



- T. J. Wallington, Degradation of Fluorotelomer Alcohols: A Likely Atmospheric Source of Perfluorinated Carboxylic Acids, *Environ. Sci. Technol.*, 2004, **38**, 3316–3321.
- 151 R. Holland, M. A. H. Khan, R. Chhantyal-Pun, A. J. Orr-Ewing, C. J. Percival, C. A. Taatjes and D. E. Shallcross, Investigating the Atmospheric Sources and Sinks of Perfluorooctanoic Acid Using a Global Chemistry Transport Model, *Atmosphere*, 2020, **11**, 407.
- 152 G. Yarwood, S. Kembal-Cook, M. Keinath, R. L. Waterland, S. H. Korzeniowski, R. C. Buck, M. H. Russell and S. T. Washburn, High-Resolution Atmospheric Modeling of Fluorotelomer Alcohols and Perfluorocarboxylic Acids in the North American Troposphere, *Environ. Sci. Technol.*, 2007, **41**, 5756–5762.
- 153 W. Sun, S. Huo, X. Zhao, G. Zhou, W. Wang and Q. Wang, The degradation mechanism of fluorotelomer alcohols (FTOHs) initiated by OH radicals in advanced oxidation process and the potential environmental risks of degradation products, *Process Saf. Environ. Prot.*, 2025, **203**, 107867.
- 154 M. F. Rahman, S. Peldszus and W. B. Anderson, Behaviour and fate of perfluoroalkyl and polyfluoroalkyl substances (PFASs) in drinking water treatment: A review, *Water Res.*, 2014, **50**, 318–340.
- 155 J. P. Giesy and K. Kannan, Peer Reviewed: Perfluorochemical Surfactants in the Environment, *Environ. Sci. Technol.*, 2002, **36**, 146A–152A.
- 156 M. Altarawneh and B. Z. Dlugogorski, in *Organohalogen Compounds*, EcoInforma Press, 2012, vol. 74, pp. 407–411.
- 157 M. H. Plumlee, K. McNeill and M. Reinhard, Indirect Photolysis of Perfluorochemicals: Hydroxyl Radical-Initiated Oxidation of N-Ethyl Perfluorooctane Sulfonamido Acetate (N-EtFOSAA) and Other Perfluoroalkanesulfonamides, *Environ. Sci. Technol.*, 2009, **43**, 3662–3668.
- 158 M. B. Blanco, I. Bejan, I. Barnes, P. Wiesen and M. a. Teruel, Atmospheric Photooxidation of Fluoroacetates as a Source of Fluorocarboxylic Acids, *Environ. Sci. Technol.*, 2010, **44**, 2354–2359.
- 159 C. E. Müller, A. C. Gerecke, C. Bogdal, Z. Wang, M. Scheringer and K. Hungerbühler, Atmospheric fate of poly- and perfluorinated alkyl substances (PFASs): I. Day-night patterns of air concentrations in summer in Zurich, Switzerland, *Environ. Pollut.*, 2012, **169**, 196–203.
- 160 P. Karásková, G. Codling, L. Melymuk and J. Klánová, A critical assessment of passive air samplers for per- and polyfluoroalkyl substances, *Atmos. Environ.*, 2018, **185**, 186–195.
- 161 A. Jahnke, L. Ahrens, R. Ebinghaus, U. Berger, J. L. Barber and C. Temme, An improved method for the analysis of volatile polyfluorinated alkyl substances in environmental air samples, *Anal. Bioanal. Chem.*, 2007, **387**, 965–975.
- 162 Y. Tian, Y. Yao, S. Chang, Z. Zhao, Y. Zhao, X. Yuan, F. Wu and H. Sun, Occurrence and Phase Distribution of Neutral and Ionizable Per- and Polyfluoroalkyl Substances (PFASs) in the Atmosphere and Plant Leaves around Landfills: A Case Study in Tianjin, China, *Environ. Sci. Technol.*, 2018, **52**, 1301–1310.
- 163 L. Vierke, L. Ahrens, M. Shoeib, E. J. Reiner, R. Guo, W.-U. Palm, R. Ebinghaus and T. Harner, Air concentrations and particle-gas partitioning of polyfluoroalkyl compounds at a wastewater treatment plant, *Environ. Chem.*, 2011, **8**, 363–371.
- 164 M. Shoeib, T. Harner, M. Ikononou and K. Kannan, Indoor and outdoor air concentrations and phase partitioning of perfluoroalkyl sulfonamides and polybrominated diphenyl ethers, *Environ. Sci. Technol.*, 2004, **38**, 1313–1320.
- 165 N. Paragot, J. Bečanová, P. Karásková, R. Prokeš, J. Klánová, G. Lammel and C. Degrendele, Multi-year atmospheric concentrations of per- and polyfluoroalkyl substances (PFASs) at a background site in central Europe, *Environ. Pollut.*, 2020, **265**, 114851.
- 166 M. Guo, Y. Lyu, T. Xu, B. Yao, W. Song, M. Li, X. Yang, T. Cheng and X. Li, Particle size distribution and respiratory deposition estimates of airborne perfluoroalkyl acids during the haze period in the megacity of Shanghai, *Environ. Pollut.*, 2018, **234**, 9–19.
- 167 Y. Yao, H. Sun, Z. Gan, H. Hu, Y. Zhao, S. Chang and Q. Zhou, Nationwide Distribution of Per- and Polyfluoroalkyl Substances in Outdoor Dust in Mainland China From Eastern to Western Areas, *Environ. Sci. Technol.*, 2016, **50**, 3676–3685.
- 168 H. Lin, S. Taniyasu, E. Yamazaki, S. Wei, X. Wang, N. Gai, J. H. Kim, H. Eun, P. K. S. Lam and N. Yamashita, Per- and Polyfluoroalkyl Substances in the Air Particles of Asia: Levels, Seasonality, and Size-Dependent Distribution, *Environ. Sci. Technol.*, 2020, **54**, 14182–14191.
- 169 X. Li, Y. Wang, J. Cui, Y. Shi and Y. Cai, Occurrence and Fate of Per- and Polyfluoroalkyl Substances (PFAS) in Atmosphere: Size-Dependent Gas-Particle Partitioning, Precipitation Scavenging, and Amplification, *Environ. Sci. Technol.*, 2024, **58**, 9283–9291.
- 170 A. Jahnke, L. Ahrens, R. Ebinghaus and C. Temme, Urban versus remote air concentrations of fluorotelomer alcohols and other polyfluorinated alkyl substances in Germany, *Environ. Sci. Technol.*, 2007, **41**, 745–752.
- 171 H. P. H. Arp, R. P. Schwarzenbach and K.-U. Goss, Ambient Gas/Particle Partitioning. 1. Sorption Mechanisms of Apolar, Polar, and Ionizable Organic Compounds, *Environ. Sci. Technol.*, 2008, **42**, 5541–5547.
- 172 S.-K. Kim, D. Li and K. Kannan, *In situ* measurement-based partitioning behavior of perfluoroalkyl acids in the atmosphere, *Environ. Eng. Res.*, 2020, **25**, 281–289.
- 173 H. Lin, S. Taniyasu, N. Yamashita, M. K. Khan, S. S. Masood, S. Saied and H. A. Khwaja, Per- and polyfluoroalkyl substances in the atmospheric total suspended particles in Karachi, Pakistan: Profiles, potential sources, and daily intake estimates, *Chemosphere*, 2022, **288**, 132432.
- 174 S. Fang, C. Li, L. Zhu, H. Yin, Y. Yang, Z. Ye and I. T. Cousins, Spatiotemporal distribution and isomer profiles of perfluoroalkyl acids in airborne particulate



- matter in Chengdu City, China, *Sci. Total Environ.*, 2019, **689**, 1235–1243.
- 175 C. Li, J. Chen, H.-B. Xie, Y. Zhao, D. Xia, T. Xu, X. Li and X. Qiao, Effects of Atmospheric Water on ·OH-initiated Oxidation of Organophosphate Flame Retardants: A DFT Investigation on TCP, *Environ. Sci. Technol.*, 2017, **51**, 5043–5051.
- 176 Z. Wang, Z. Xie, A. Möller, W. Mi, H. Wolschke and R. Ebinghaus, Estimating dry deposition and gas/particle partition coefficients of neutral poly-/perfluoroalkyl substances in northern German coast, *Environ. Pollut.*, 2015, **202**, 120–125.
- 177 B. Sha, J. H. Johansson, M. E. Salter, S. M. Blichner and I. T. Cousins, Constraining global transport of perfluoroalkyl acids on sea spray aerosol using field measurements, *Sci. Adv.*, 2024, **10**, ead11026.
- 178 G. Casas, A. Martínez-Varela, J. L. Roscales, M. Vila-Costa, J. Dachs and B. Jiménez, Enrichment of perfluoroalkyl substances in the sea-surface microlayer and sea-spray aerosols in the Southern Ocean, *Environ. Pollut.*, 2020, **267**, 115512.
- 179 Overview, <https://chm.pops.int/Implementation/IndustrialPOPs/PFAS/Overview/tabid/5221/Default.aspx>, accessed 13 November 2025.

